Bulletin of the Seismological Society of America, Vol. 94, No. 6B, pp. S23–S52, December 2004

Ⓔ

Surface Rupture and Slip Distribution of the Denali and Totschunda Faults in the 3 November 2002 **M** 7.9 Earthquake, Alaska

by Peter J. Haeussler, David P. Schwartz, Timothy E. Dawson, Heidi D. Stenner, James J. Lienkaemper, Brian Sherrod, Francesca R. Cinti, Paola Montone, Patricia A. Craw, Anthony J. Crone, and Stephen F. Personius

Abstract The 3 November 2002 Denali fault, Alaska, earthquake resulted in 341 km of surface rupture on the Susitna Glacier, Denali, and Totschunda faults. The rupture proceeded from west to east and began with a 48-km-long break on the previously unknown Susitna Glacier thrust fault. Slip on this thrust averaged about 4 m (Crone *et al.*, 2004). Next came the principal surface break, along 226 km of the Denali fault, with average right-lateral offsets of 4.5–5.1 m and a maximum offset of 8.8 m near its eastern end. The Denali fault trace is commonly left stepping and north side up. About 99 km of the fault ruptured through glacier ice, where the trace orientation was commonly influenced by local ice fabric. Finally, slip transferred southeastward onto the Totschunda fault and continued for another 66 km where dextral offsets average 1.6–1.8 m. The transition from the Denali fault to the Totschunda fault occurs over a complex 25-km-long transfer zone of right-slip and normal fault traces. Three methods of calculating average surface slip all yield a moment magnitude of M_w 7.8, in very good agreement with the seismologically determined magnitude of **M** 7.9. A comparison of strong-motion inversions for moment release with our slip distribution shows they have a similar pattern. The locations of the two largest pulses of moment release correlate with the locations of increasing steps in the average values of observed slip. This suggests that slip-distribution data can be used to infer moment release along other active fault traces.

Online Material: Descriptions and photographs of localities with offset measurements.

Introduction

The **M** 7.9 Denali fault earthquake of 3 November 2002 was the largest strike-slip earthquake in North America in almost 150 years and produced effects felt up to 3500 km from the epicenter (Eberhart-Phillips *et al.*, 2003). It was also one of a few **M** 7.8 or larger strike-slip earthquakes in shallow continental crust worldwide in the past century. The scarcity of such earthquakes deems them worthy of study, particularly as analogs for the San Andreas and associated large strike-slip faults in California. This article describes the surface rupture and slip distribution of the Denali and Totschunda faults, the two primary strike-slip faults that ruptured in the 2002 Denali fault earthquake (Fig. 1). An accompanying article by Crone *et al.* (2004) discusses the surface rupture of the Susitna Glacier thrust fault, along which the earthquake sequence started.

The Denali fault earthquake occurred on a system of active intracontinental faults that accommodate part of the oblique collision of the Yakutat terrane into the southern Alaska margin (Fig. 1). The Denali fault is a major right-lateral strike-slip fault, with at least 38 km of offset in the past 38 Ma (St. Amand, 1957; Grantz, 1966; Reed and Lanphere, 1973; Brogan *et al.*, 1975). Richter and Matson (1971) defined the associated Totschunda fault on a regional scale, identified evidence of Holocene offset, and proposed that it transfers strain west of the Fairweather fault onto the Denali fault system. Active thrust faults have been identified and postulated on both the north and south sides of the Alaska Range (St. Amand, 1957; Weber and Turner, 1977; Thoms, 2000; Ridgeway *et al.*, 2002; Bemis and Wallace, 2003). A map of stress orientations across Alaska (Plafker *et al.*, 1994) shows compression across the Denali fault. These relationships all indicate transpression across the right-lateral Denali fault system with associated thrust faults accommodating shortening.

On 23 October 2002, the **M** 6.7 Nenana Mountain earthquake occurred on the Denali fault, ~22 km west of the epicenter of the 3 November 2002 mainshock (Fig. 1). This foreshock had a focal mechanism that showed right-lateral

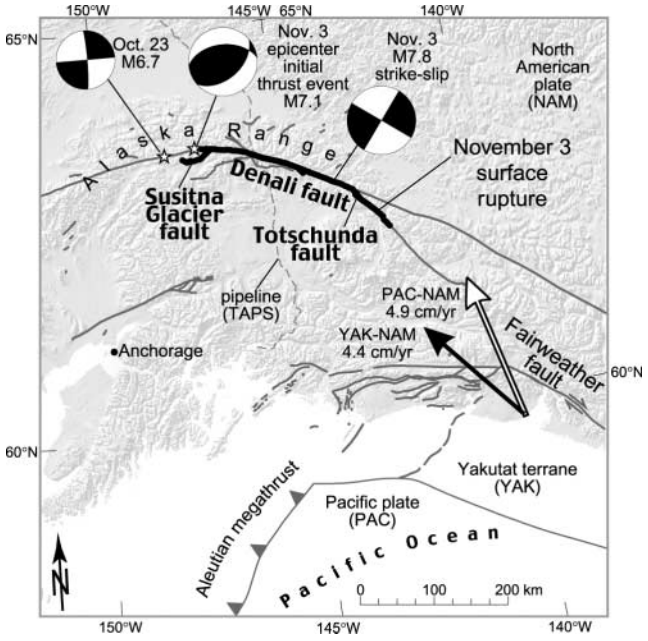

Figure 1. Map showing tectonic setting of the Denali and Totschunda faults. Active faults are shown with gray lines (Plafker *et al.*, 1994), and the 2002 Denali fault earthquake surface rupture is shown with thick black lines. Locations of the 23 October and 3 November 2002 epicenters are shown as stars. The GPS-measured motion of Yakutat relative to Fairbanks, Alaska, is shown with the solid black arrow (Fletcher and Freymueller, 1999). The relative motion between the Pacific plate and North America is shown with the white arrow (DeMets *et al.*, 1994). TAPS refers to the Trans-Alaska Pipeline System.

strike slip, and aftershocks extended both east and west along the Denali fault (Eberhart-Phillips *et al.*, 2003). We flew over the epicentral region the day of the earthquake and observed abundant rockfall and snow avalanches, but no surface rupture. Modeling of Radarsat interferograms with a best-fit dislocation model indicates a 21-km-long rupture patch, with about 0.9 m of right-lateral slip below 4 km deep and ≤0.2 m above 4 km (Wright *et al.*, 2003).

The 3 November 2002 **M** 7.9 earthquake was produced by west to east rupture along three faults (Fig. 2A; Eberhart-Phillips *et al.*, 2003). The rupture began with thrust faulting on a 48-km-long break of the previously unrecognized Susitna Glacier fault. Dip slip on this fault was estimated from scarp heights to average 4.0 m (Crone *et al.*, 2004). Rupture then occurred along 226 km of the Denali fault, where right-lateral slip at the surface averaged 4.5–5.1 m and reached a maximum of 8.8 m. Finally, the rupture progressed southeasterly another 66 km along the Totschunda fault, where right-lateral surface offsets averaged ~1.7 m.

Strong-motion studies show there were three pulses of moment release during the earthquake. First, there was a **M** 7.1 pulse from the Susitna Glacier fault; second, there was a **M** 7.0 pulse from a small region 90–100 km east of the epicenter (near the Trans-Alaska Pipeline System [TAPS] crossing); third, there was a **M** 7.6 pulse from the broad region 160–230 km east of the epicenter (Frankel, 2004). These conclusions are broadly supported by Global Positioning System (GPS) geodetic data (Eberhart-Phillips *et al.*, 2003; Hreinsdóttir *et al.*, 2003a,b). In all, the rupture took about 100 sec.

Observations of the 2002 Surface Rupture

Timing of Observations

In general, mapping of surface rupture and measurement of offsets are best made immediately after an earthquake when fragile and ephemeral structural and geomorphic features are fresh. Observations of the Denali and Totschunda surface rupture were made during two main field efforts, the first in November 2002 immediately after the earthquake and the second in July 2003 (Figs. 3, 4, and 5; Appendix 1, 2; http://quake.wr.usgs.gov/research/seismology/alaska/). A few additional observations were made in July 2004. In 2002, we observed and measured the surface rupture on 4 and 5 November and then from 7 through 12 November. Fortunately, little snow fell along the surface trace during our November postearthquake investigations. In 2003, we collected data from 16–25 July. In 2004, we made observations from 2 to 8 July. Almost all locations required helicopter access.

Observing the fault ruptures at different times proved to be advantageous because some features were best seen under frozen, November conditions, and others were more distinct without snow cover. In November 2002 there was typically 20–80 cm of snow cover and the fault rupture appeared as distinct dark-brown gaps in the white snow pack (Fig. 3A–C). Some of the snow along the fault trace was firm névé and some was powder. The névé was brittle, attached to the ground surface, and ground cracks with extension as small as 1 cm were discernible. We believe thin-powder snow may have obscured ruptures having slip of less than about 10 cm. The firm snow cover made the fine-scale details of the surface rupture obvious and measurement of some offsets simple. Conversely, it was difficult to determine whether some features in the snow were due to drifting, natural snow variations, or fault offset. Measurements made in November 2002 on offsets of glacier ice could not be repeated in July 2003, because the melting of glacier ice, collapse of cracks and crevasses, and the infilling of the fault trace with winter snow largely obliterated offset features. However, at some locations below the firn line, glacier surfaces observed in July 2003 revealed snow-filled crevasses offset across the fault (Fig. 4C,D).

In July 2003, permafrost exposed in fault fissures had largely melted, which resulted in degradation of some features observed in November, and those offset measurements could not be repeated. However, without snow in July, there were many additional fine-scale features of the fault trace

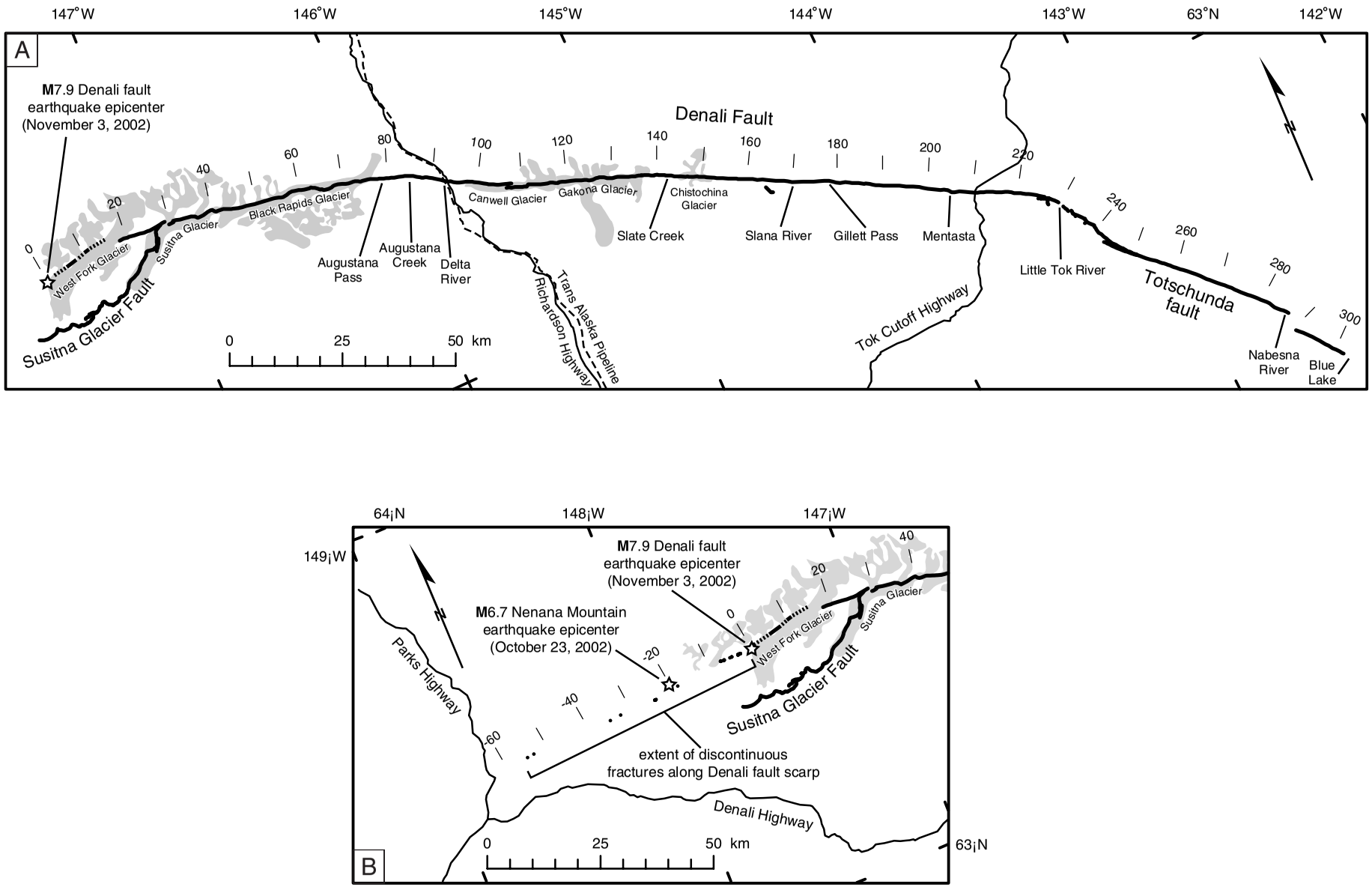

Figure 2. Maps of the 3 November 2002 surface rupture. Continuous surface rupture shown with black line. Dot-dashed line at west end shows extent of ground cracks observed in the summer of 2003 on high mountain ridges north of West Fork Glacier. Glaciers are shown in light gray. Distances east of the epicenter are in kilometers. (A) Map of continuous surface rupture. (B) Map of discontinuous fractures along the Denali fault trace west of the epicenter of the 3 November 2002 Denali fault earthquake observed in July 2004 (see text).

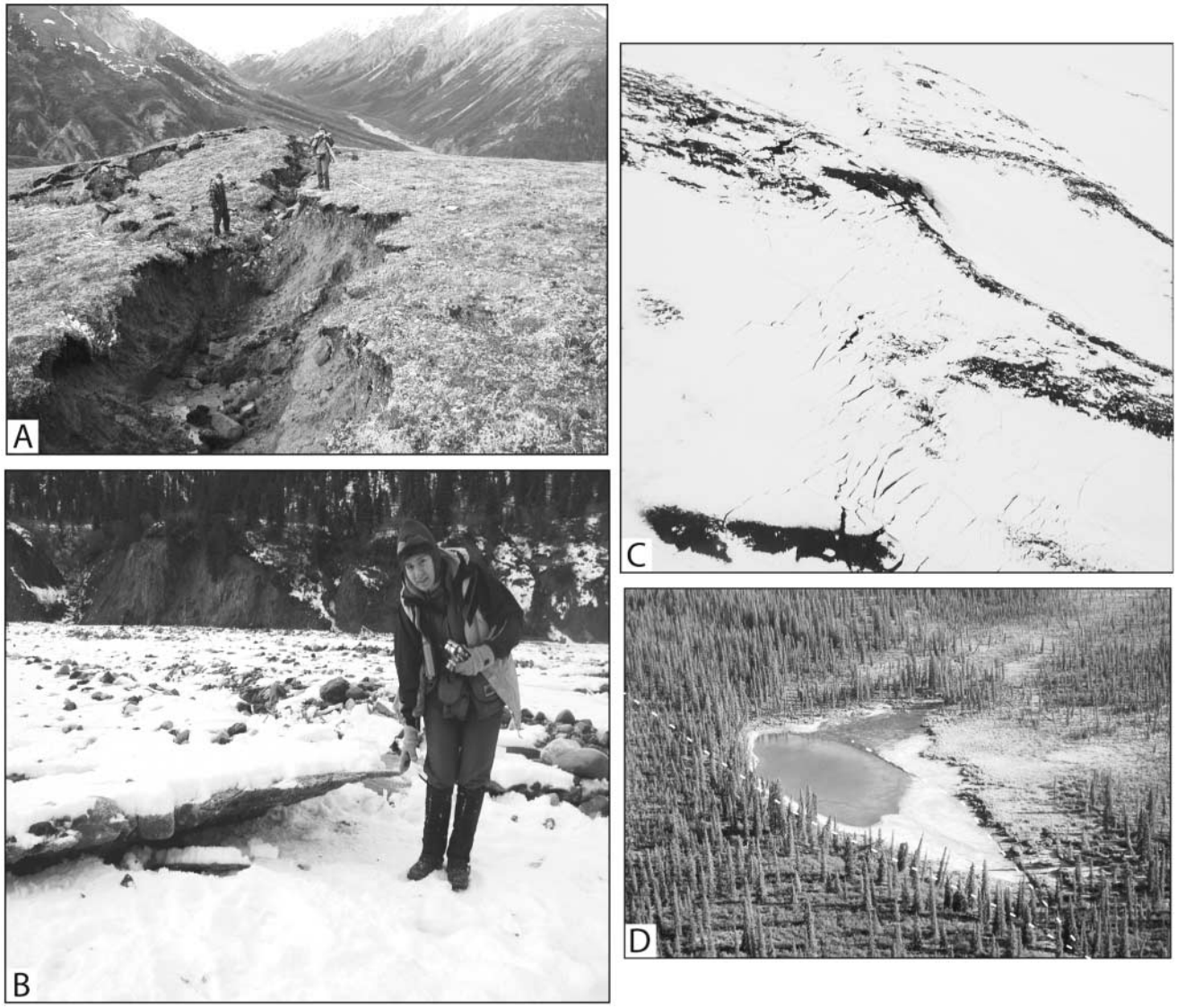

Figure 3. Photographs of features of the Denali and Totschunda fault rupture, where "on land" (i.e., not on glaciers). (A) View of the Denali fault rupture at the pass west of the Delta River (km 89). Steep walls at the bottom of the fissure are permafrost. These walls had degraded significantly by July 2003. View is toward the west. (B) Overthrusting of frozen river gravels at Cooper Creek at the southeastern end of the Totschunda fault, at km 297. (C) Left-stepping, en echelon Riedel shears in snow along the Denali fault indicate right-lateral shear. Aerial view to the east, at about km 78, on the west side of Augustana Pass. (D) Aerial view of large sag pond in the transfer zone between the Denali and Totschunda faults at km 235.5. White dashed line shows locations of fault traces. (*continued*)

that were covered by the November snowpack. Offset thalwegs, channel margins, and ephemeral stream-bank edges were clear in the summer (Fig. 5).

General Features of the Surface Rupture

Surface rupture from the 2002 Denali fault earthquake extended 341 km (Table 1; Fig. 2). The principal strike-slip rupture accompanying the 2002 earthquake is a 218-km break that reoccupied older fault scarps along the Denali fault (Fig. 3D–H). To simplify discussion, locations along the fault will be referred to by their distance east of the National Earthquake Information Center (NEIC) determined epicenter, which was the direction of rupture propagation (e.g., km 68 is 68 km east of the epicenter; negative values are west of the epicenter). The western terminus of the continuous rupture mapped in November 2002 is about 19 km east of the epicenter and 10 km west of the intersection of the Denali and Susitna Glacier faults (Fig. 2A). Between km 5 and 17, off-fault ruptures with right-lateral offset were

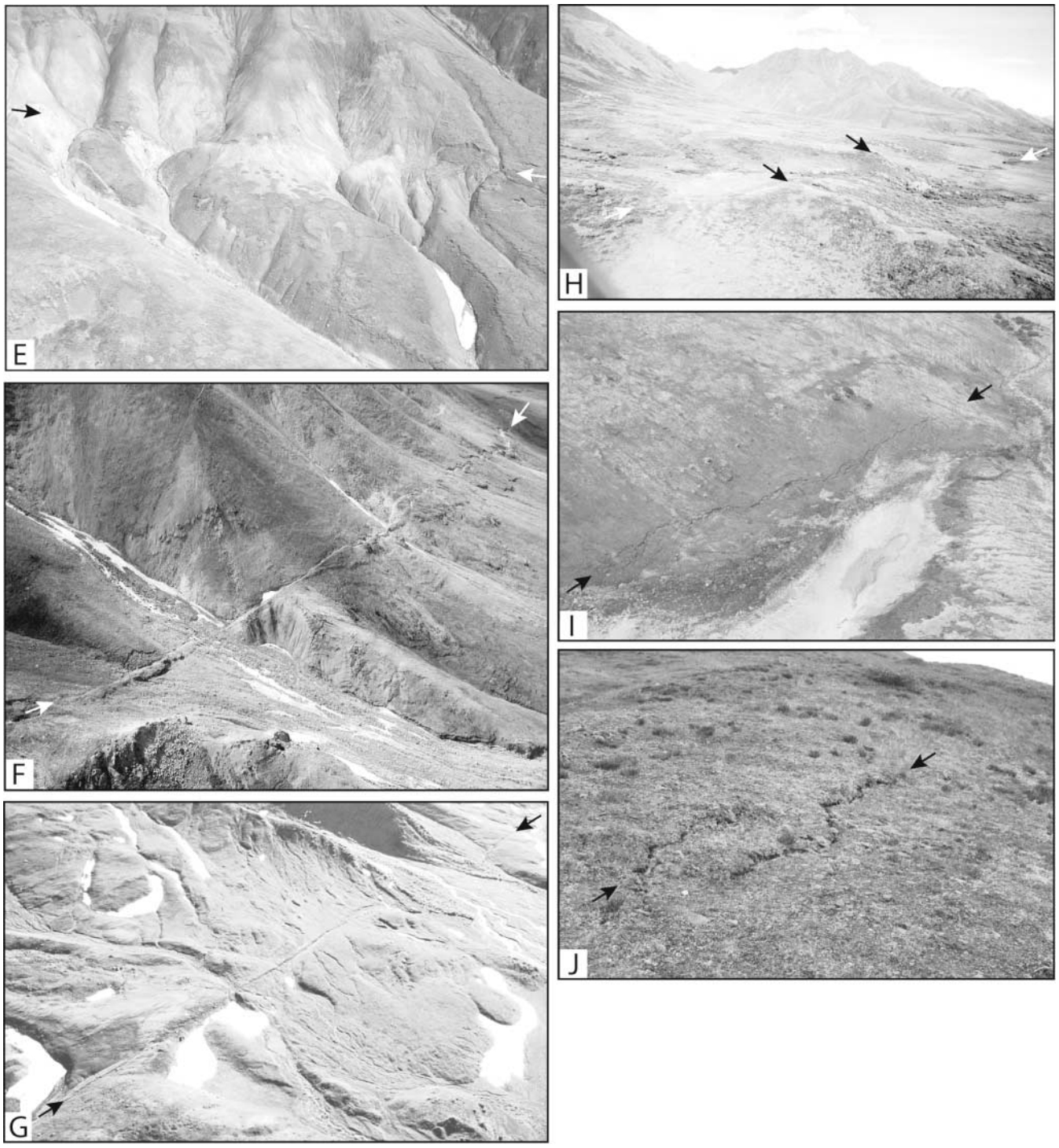

Figure 3. (*Continued*) (E) Aerial view of multiple offset gullies near Augustana Pass (km 80). Arrows point along fault trace, and the view is to the north. (F) The Denali fault trace on the west side of Gillett Pass dips about 76° to the west, at about km 178. (G) Aerial view of the narrow Denali fault rupture in the Slate Creek area, at about km 143. Arrows point along fault trace. (H) Aerial view of long-term offset of about 170 m (measurement from A. Matmon, unpublished) of linear moraine edge (black arrows) along the Denali fault (white arrows), at km 153. (I) Aerial view to the west of ground cracks along part of the Denali fault scarp 18 km west of the 2002 epicenter. The cracks are about 50 m long and lie along the pre-existing scarp. The block at the bottom right side (the north side) slid downhill as indicated by extensional cracks. (J) View of discontinuous ground cracks from the ground. These two cracks, at km −4.6, lie along the Denali fault scarp, are approximately 7 m long, and had about 4 cm displacement in the downslope direction.

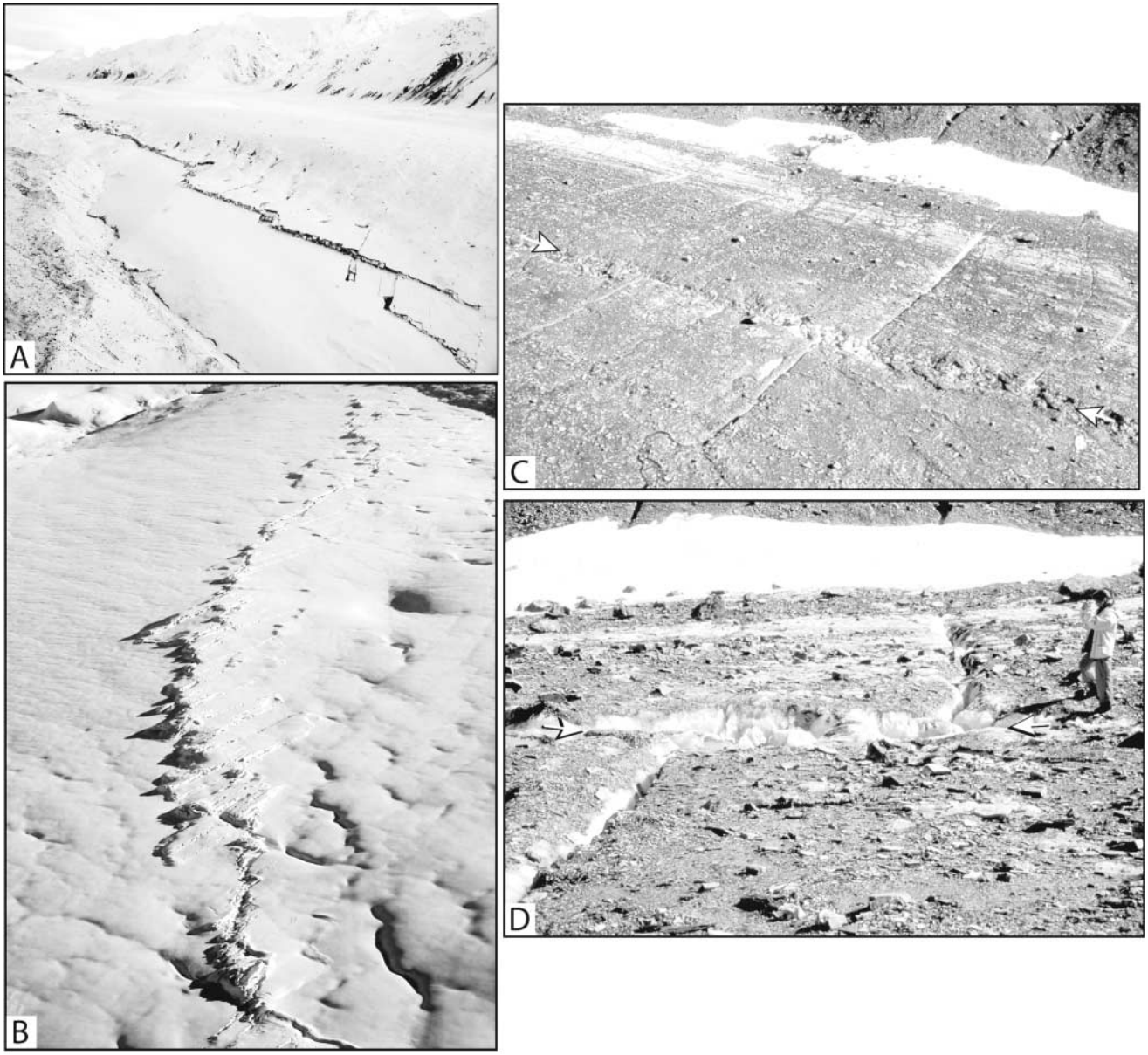

Figure 4. Photographs of features along the Denali and Totschunda fault rupture, where "on glaciers" (i.e., propagated through glacier ice). (A) Aerial view westward of the Denali fault trace along the northern margin of the Canwell Glacier, at about km 100, 3 November 2002. (B) Aerial view in November 2002 of complex fault rupture in the Gakona Glacier at about km 133. Note numerous Riedel shears that are nearly perpendicular to snow-filled crevasses. It was not possible to find features to measure across fault traces like this in November 2002. (C) Aerial view of offset crevasses in the Chistochina Glacier at km 147.7 in July 2003. Arrows point along fault trace, which is linear and narrow across this glacier. Close-up of prominent offset crevasse in the photo's center is shown in D. (D) Offset crevasse (4.6 ± 0.1 m lateral, 0.3 ± 0.05 m vertical displacement) in the Chistochina Glacier, km 147.7, July 2003. Arrows point along fault trace. (*continued*)

observed from the air. West of the epicenter there are discontinuous ground cracks that lack lateral offset (with two exceptions that had less than 5 cm offset at km −1.25 and km −34.95), generally occur in wet areas, and are sometimes associated with sand blows (Fig. 3I,J). These fractures were observed along a 33.7-km-long section of the Denali fault trace from km −1 to km −35 (Fig. 2B; Appendix 2). These fractures, which were observed in July 2003 and July 2004, lie mainly between the epicenters of the October and November 2002 earthquakes (Fig. 2B). Because it is uncer-

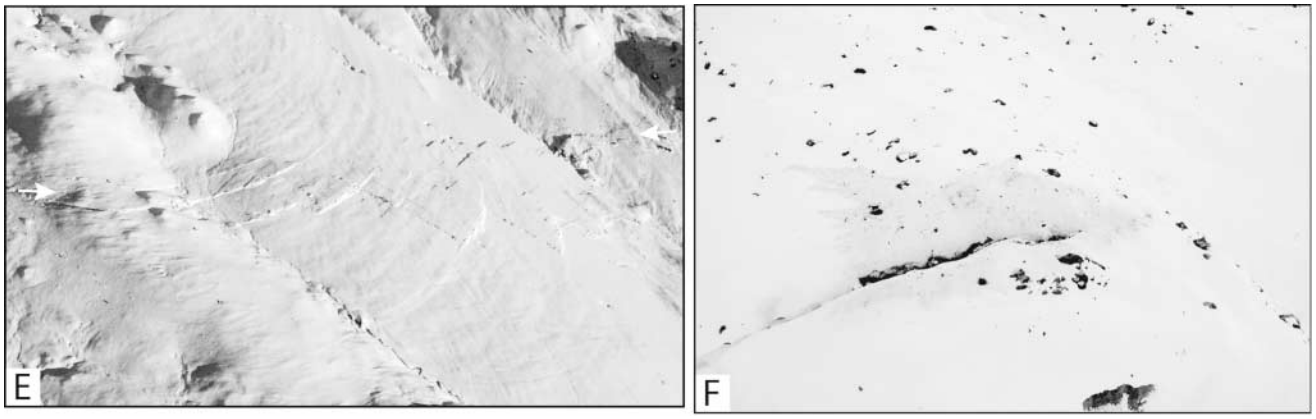

Figure 4. (*Continued*) (E) Aerial view to the east in November 2002 of fault trace (between arrows) crossing a narrow glacier with ogives (ice waves perpendicular to flow direction), at about km 140. Note that the fault trace includes strands parallel to the ogive bands and others nearly perpendicular to the bands that connected the two. This demonstrates the influence of the ice fabric on the surface trace. (F) Aerial view in November 2002 of ice and snow that was apparently exhaled from the adjacent crevasse during the earthquake. Location is near the intersection of the Susitna Glacier and Denali fault at about km 29. Width of debris on glacier is approximately 15 m.

tain during which of these events they formed, or whether they represent shaking or incipient surface faulting, they are not included in the overall length of the 2002 surface rupture.

The Denali surface rupture was typically a single break, without splays or parallel traces. Previously, we reported a 6-km-long west-northwest-striking rupture south of the Denali fault near km 160 (Eberhart-Phillips *et al.*, 2003). This strand was re-evaluated in the field and on aerial photographs. We found no direct connection to the Denali fault, and the length is 2.1 km (Fig. 2A). The rupture exhibits downslope extension and lies at the base of the southern side of a high ridge that has numerous sackungen. It may be shaking related, but because of its occurrence on the flats south of the ridge, we cannot preclude a tectonic origin.

The Denali fault did not break east of its intersection with the Totschunda fault (Figs. 2A, 6D). There is, however, geomorphic expression of Holocene faulting farther southeast along the Denali fault (Richter and Matson, 1971; Clague, 1979). At the eastern limit of the 2002 rupture on the Denali fault surface faulting stepped 17° southeastward onto the Totschunda fault across a complex, 26-km-long transfer zone (Figs. 2A, 6D). The transfer zone from the Denali to the Totschunda faults has a series of right-stepping fault segments that are connected by north-striking east-side-up normal faults with displacements as large as 2.7 m, and a 7.9-km-long splay parallel to the main trace of the Totschunda fault at the southeastern end of the transfer zone. The Totschunda fault surface ruptures extend a total of 66 km southeastward along the fault. Two strands of the Totschunda fault ruptured: the longer Totschunda Creek strand (32.6 km) and the shorter Cooper Pass strand (8.5 km). Surface rupture along the two strands is separated by a 4.2-km right step.

The on-land (not through glacier ice) surface trace of the Denali fault typically consisted of en echelon left steps (Fig. 6B). Individual rupture segments extended for a few tens of meters to hundreds of meters in length, commonly as a narrow-mole-track one to a few meters wide (Figs. 3 and 5). The zone of rupture broadened and was more structurally complex at the step-overs between the individual segments. Where we have detailed rupture maps (i.e., Fig. 6), the distance between segments is typically 5–9 m and up to 21 m. Within these step-over zones, local changes in fault geometry result in formation of both pressure ridges and graben. In contrast to the Denali fault, the Totschunda fault has significantly fewer steps, either left or right (Fig. 6E).

Surface Rupture Through Glaciers

About 99 km of the surface rupture passed through glacier ice, where the rupture pattern was often wide and commonly influenced by the ice fabric (Fig. 4A,B,E). The surface rupture was usually expressed as a jagged linear trace, with numerous small displacement cracks radiating outward at fairly consistent angles (Fig. 4A,B). Some cracks appeared parallel to the ice fabric where bare ice or a cross section of the ice could be seen. This pattern was common on the Chistochina and parts of the Gakona, Black Rapids, and Susitna Glaciers. The surface trace was locally parallel to medial moraines on the Susitna, Black Rapids, and Gakona Glaciers. Sections of the surface break were parallel to the ice fabric in ogives, clearly demonstrating the influence of ice fabric on the surface trace (Fig. 4E). Right steps in the fault trace resulted in pull-aparts of various scales (Fig. 4A). An unusual feature was observed on the Susitna Glacier in November 2002, near the intersection between the Susitna

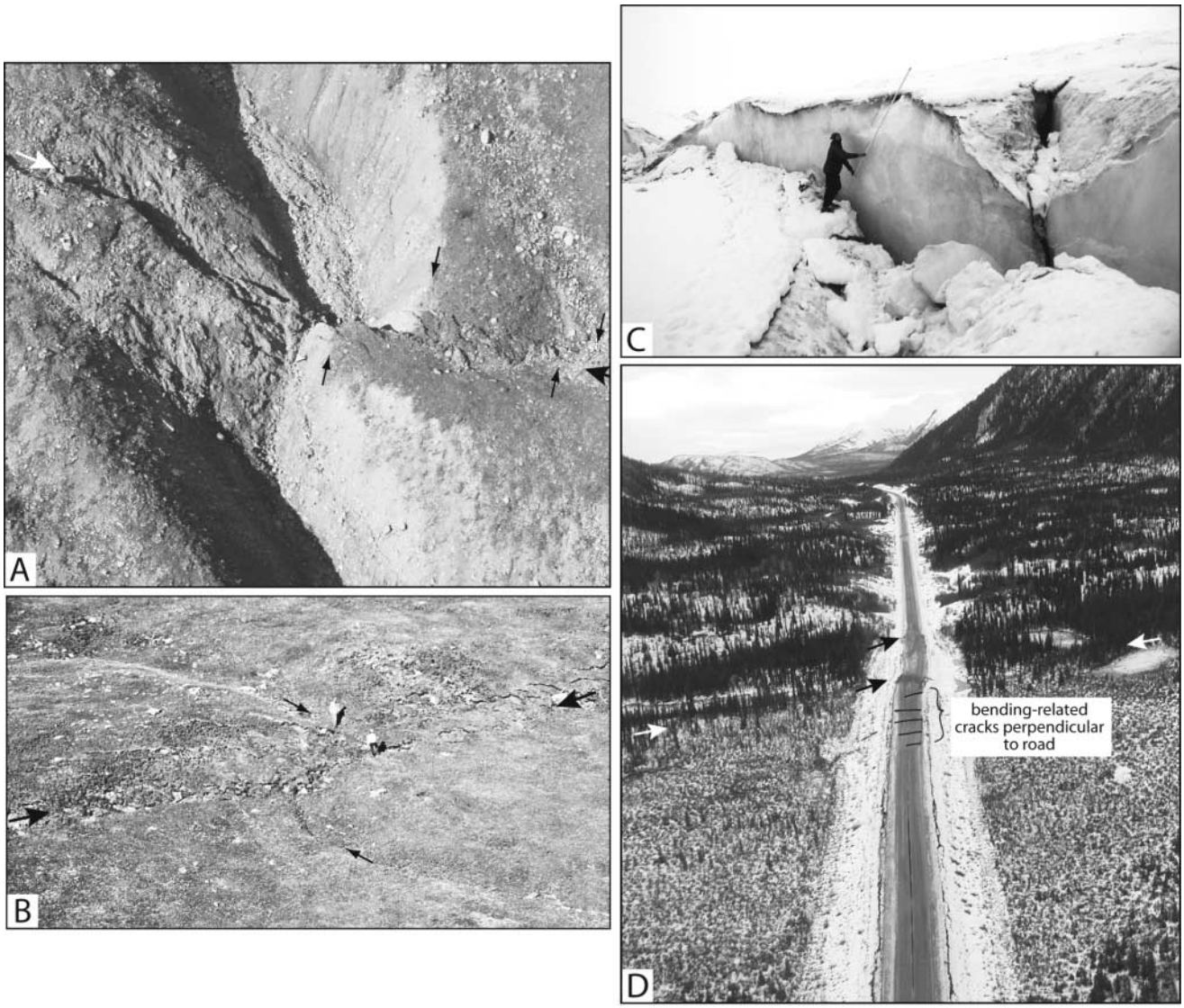

Figure 5. Photographs of offset features measured along the Denali and Totschunda fault traces. (A) Mountainside channel at km 138.6 with 7.2 + 0.7/−0.8 m of offset (small arrows at center). The gravelly swale at the right of the photo was offset 3.7 + 0.6/−0.5 m (small arrows at right). We interpret the 7.2-m displacement as a result of two earthquakes. Large arrows point along the fault trace. (B) Offset channel at km 143.52, near Slate Creek. Large arrows point along the fault rupture, small arrows point to the 4.8 ± 0.5 m offset. (C) Offset crevasse along northern margin of Canwell Glacier at km 102.9. This locality had 3.52 m right-lateral slip and 2.05 m south-side-up vertical slip, which was the largest measured vertical slip of any "on-glacier" locality. (D) Southward-looking aerial view of the Tok Cutoff Highway (km 210.6) offset by two strands of the Denali fault (arrows). Note the fractures perpendicular to the road, accommodating bending. Five meters of offset occurred across the main two fault traces, and 6.9 m of offset occurred across the entire rupture zone. (*continued*)

Glacier and Denali faults. At this location, freshly deposited snow and ice in a ~20-m-wide zone surrounding a crevasse appears to have been exhaled from the crevasse during the earthquake (Fig. 4F). Figure 6A shows a detailed surface trace map of the west end of the Denali fault trace based on georeferenced aerial photographs. On the Susitna Glacier, the zone of deformation is up to 941 m wide along the Denali fault, whereas the adjacent fault trace on land is typically less than 9 m wide between overlapping en echelon strands. The Susitna Glacier thrust fault trace was up to 1420 m wide on the Susitna Glacier (Fig. 6A).

At some locations the rupture zone through glacier ice is narrow. For example, along the northern margin of the Canwell Glacier, around km 100 (Fig. 4A), the fault offset

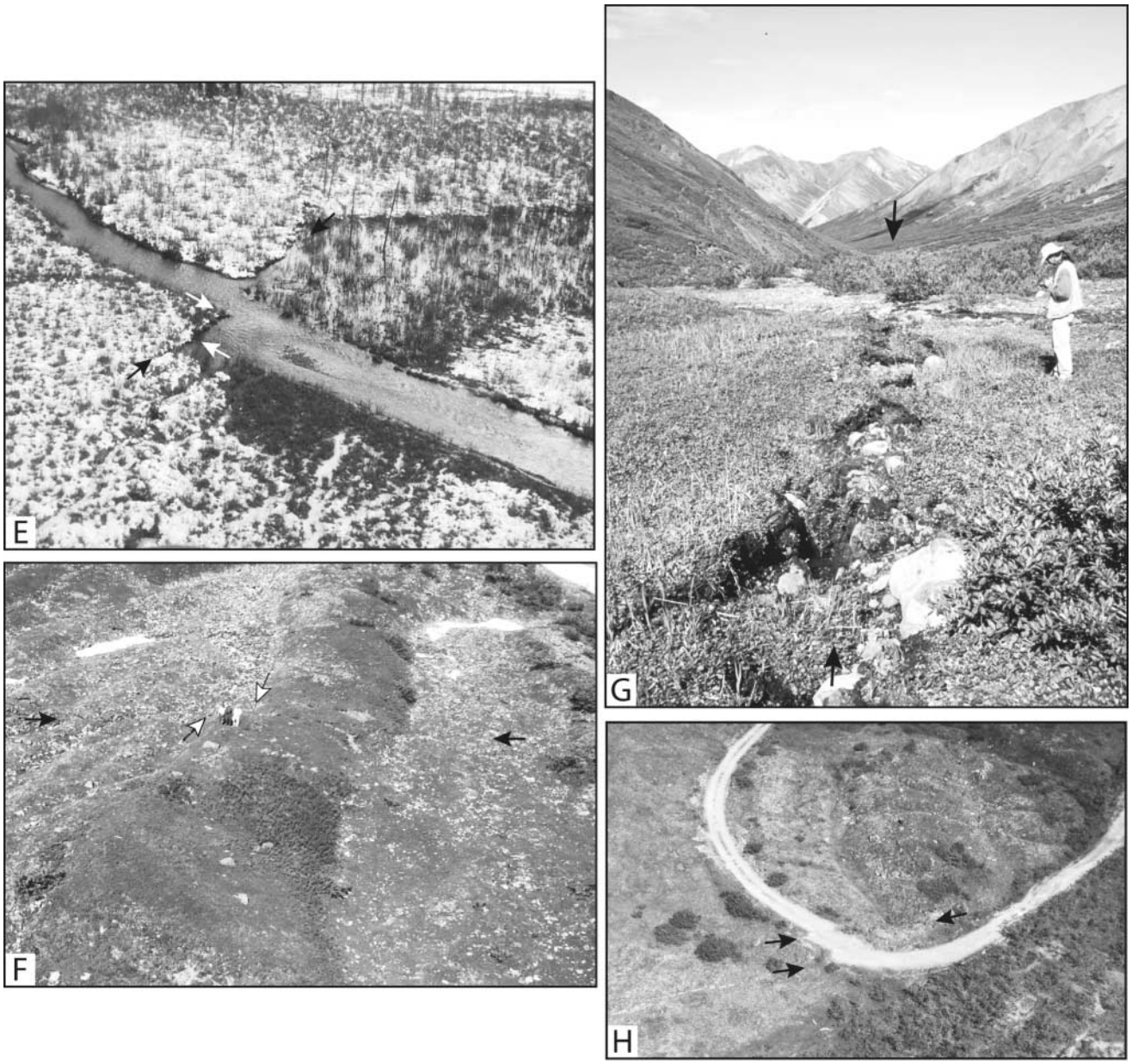

Figure 5. (*Continued*) (E) Aerial view of Bone Creek at km 192, taken in November 2002. The northwest side of the stream channel is offset by the Denali fault (black arrows). The offset (white arrows) was measured at 5.5 ± 0.1 m in November 2002 and 6.6 + 0.4/−0.5 m in July 2003. (F) View looking north at an offset terrace riser in a debris-flow-cut gully at km 143.22. The riser is offset 4.9 + 0.7/−0.45 m across a 2-m-wide zone of rupture (white arrows). Arrows point along fault trace. Note three people, for scale, between white arrows. (G) Very narrow, 1 m-wide Denali fault mole track at km 184.27, where fault has offset a creek bank 8.1 m in middle of photo (offset not visible). Arrows point along the mole track. View is to the west. (H) A dirt road at km 163.54 offset 3.6 to 4.9 m across a 4- to 5-m-wide Denali fault zone (arrows).

(*continued*)

crevasses along a zone of deformation less than one meter wide. At the eastern end of the Black Rapids Glacier, between km 68 and 74 where the fault is near the southern margin of the glacier, the rupture zone appeared less than one meter wide. Similarly, on the Chistochina Glacier at km 147 the rupture was expressed as a narrow (2-m-wide) linear mole track, up on the north, that offset crevasses and had the same geomorphic expression as the rupture on land. Visible evidence of rupture through glacier ice had disappeared by August 2004.

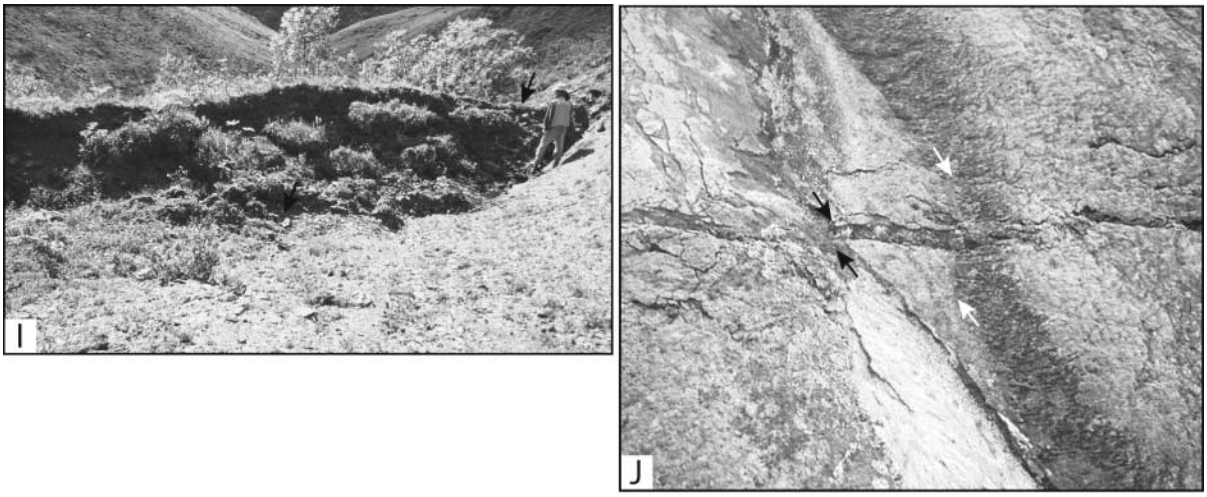

Figure 5. (*Continued*) (I) Offset gully (arrows) at km 186.19. A right-lateral displacement of 8.0 ± 0.8 m and 1.5 ± 0.2 m of vertical offset has caused the gully to be entirely blocked. (J) Offset channel margin along the Totschunda fault at km 249.9. Black arrows point to the offset from the 2002 event, which had 2.8 + 0.2/−0 m right-lateral offset. The white arrows point to a longer-term displacement of 5.6 m from two or more events.

Table 1
Denali Fault Earthquake Surface Rupture Length Measurements

Fault or Segment	Length (km)
Susitna Glacier fault	
Total	48.4
Arc of main trace with continuous rupture	42.7
Discontinuous trace at west end	5.7
Denali fault	
Total	225.6
Continuous rupture	217.6
Distance along westernmost discontinuous cracks (not included in total)	33.7
Distance along cracks on steep mountainsides along West Fork Glacier	7.0
Short strand near Gillett Pass (not included in total)	2.1
Totschunda fault	
Total (including transfer zone)	66.5
In transfer zone	21.2
Southern splay at southeast end of transfer zone (not included in total)	7.9
Totschunda Creek strand southeast of transfer zone	32.6
Link between Totschunda Creek and Cooper Pass strands	4.2
Cooper Pass strand of Totschunda fault	8.5
Total rupture length	340.5

Fault Intersections

The 2002 rupture occurred on three connected faults, which required the rupture to span intersections between the Denali and Susitna Glacier faults and between the Denali and Totschunda faults (Figs. 2, 6A, 6D). At the surface, the projection of the the Susitna Glacier thrust fault intersects the Denali fault at an angle of about 48°. Surface traces associated with each fault tend to parallel medial moraines. These ruptures do not actually intersect, but they lie within about 400 m of one another. The two faults likely intersect at depth.

The Denali-Totschunda fault intersection has a 17° change in the large-scale strike between the two fault systems; the Denali fault strikes 120° and the Totschunda fault strikes 137°. This right bend between the Denali fault and the Totschunda fault is a zone of transtension that we refer to as the transfer zone. For much of the 26-km-long transfer zone, the Totschunda fault strikes more southeasterly at 153°. Between km 226 and 250, the 2002 rupture is a complex zone of strike-slip and normal faults (Figs. 2, 6D). There are no significant lateral jumps or gaps in surface faulting between the Denali and Totschunda fault systems (Fig. 6D).

Other Features of the Surface Rupture

The 2002 surface rupture on the Denali and Totschunda faults reoccupied pre-existing fault scarps (Fig. 3E,F,G,H). It occurred in the same location as many previous surface ruptures, as shown by large-scale right-lateral offsets of moraines and drainages on the Denali fault of up to about 180 m (Fig. 3H). At one location (km 23), there was a series of en echelon step-overs where the slip could be seen to be at a maximum in the middle of each ~20- to 50-m-long fault section and then decreases toward the ends of each segment. Here gullies were offset double the amount of the 2002 rupture, indicating the 2002 offset repeated the amount of slip in the prior event (Schwartz *et al.*, 2003). The 2002 rupture also reoccupied well-developed scarps and sag ponds in the

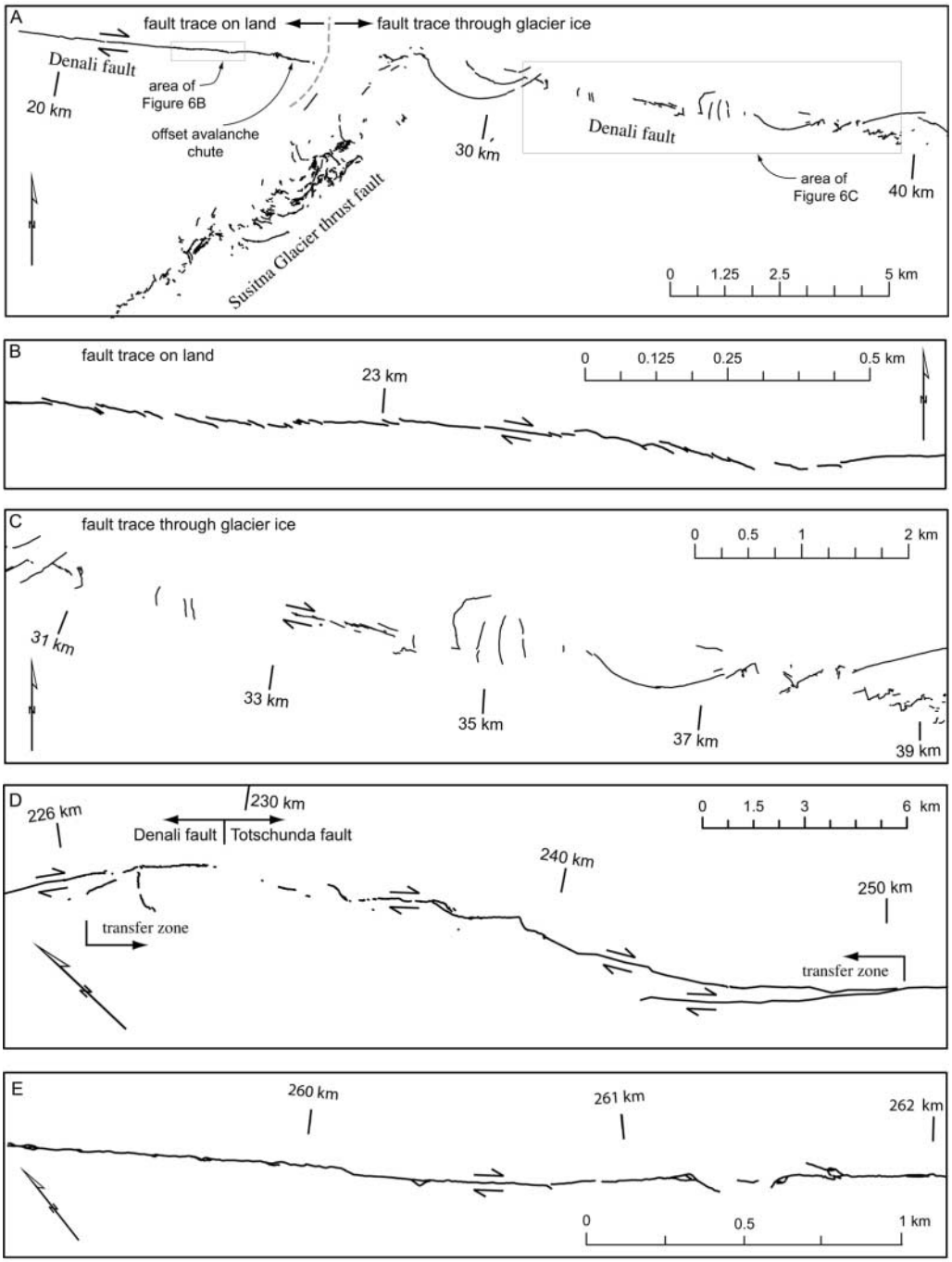

Figure 6. Detailed maps of the 2002 fault rupture at selected localities. Kilometer values refer to distance east of the epicenter as shown on Figure 2. (A) Overview of surface rupture at the west end of continuous rupture on the Denali fault and at the junction of the Susitna Glacier fault and the Denali fault. The junction between the two faults lies within or beneath glacier ice and traces from one fault do not cut across the other. (B) Detail of typical 2002 Denali fault trace on land. Location of map shown in A. Note linear trace with common left steps. (C) Detail of 2002 Denali fault trace through glacier ice along Susitna Glacier. Location shown in A. (D) 2002 fault trace in the transfer zone between Denali and Totschunda faults. (E) Detailed map of 2002 Totschunda fault surface rupture.

transfer zone (e.g., at km 235.5) between the Denali and Totschunda faults (Fig. 3D). The presence of these scarps and sag ponds indicates the transfer zone has failed in a similar way during previous earthquakes.

Snow avalanches were common along the fault trace and, in all locations except one, covered the fault scarp (Fig. 7A). They were presumably triggered by ground shaking generated as the rupture passed individual avalanche chutes. Avalanche debris was offset by the fault at only one location, which was at km 25.3. The debris in the chute appeared as fresh as an adjacent one that covered the fault. The offset avalanche debris (Figs. 6A, 7B, 7C) may have been triggered either by a magnitude 4.4 foreshock that occurred 3.5 hr before the mainshock or by shaking from the earliest stages of rupture on the main Denali fault.

The Denali fault was observed to be subvertical at most locations. For example, the fault trace between the Susitna Glacier and West Fork Glacier (between km 19 and 27) is dipping steeply to the north at roughly 80°, based on photogrammetric mapping of the fault trace. In contrast, on the west side of Gillett Pass at a ~50-m left step of the fault trace around km 175, we observed the fault dipping about 76° to the southwest. As a result, the slip was oblique with both normal and right-lateral components (Fig. 3F).

Slickensides were found at only two locations along the fault trace. On the Canwell Glacier at km 108.3, slickenlines were present on a ~1.25-m^2 face associated with an extensional step-over, about 5 m below the glacier surface (Fig. 8A). There was an estimated 1- to 2-cm-thick opaque white layer on the surface that had subhorizontal slickensides. A second site along the Totschunda fault at km 239.0 had slickensides in permafrost that first dipped 70° to the southeast and then abruptly became horizontal (Fig. 8B). Guatteri and Spudich (1998) have shown that fault slip at low stress can result in curved slickensides.

Slip Distribution Along the 2002 Surface Rupture

Offset Measurements and Uncertainties

Here we report our best effort to measure the net horizontal and vertical slip, and their uncertainties, across the primary surface rupture. Slip was measured at a total of 127 locations (Figs. 9, 10, Appendix 1). [Ⓔ Additional photographs and descriptions of most of the measured localities are available online at the SSA Web site.] Seventy-eight points were measured in November 2003, 49 points in July 2003, and 6 points in July 2004. Twenty-four points were removed from the set of 127 points (open circles, Fig. 9). The culling of these points from the slip distribution occurred where observers noted significant ground cracking away from the measured offset (thereby indicating a clear underestimate of total slip), or they considered nearby (<0.5 km away) measurements as more straightforward (structurally simple sites containing the complete rupture zone), or they could not replicate the prior offset value with repeat measurements under better summer field conditions.

Numerous types of features provided piercing points to measure vertical and lateral offsets. These included stream channels, channel banks, channel levees, channel thalwegs, terrace risers, debris-flow margins, vegetation lines paralleling stream banks, roads, tree roots, game trails, split cobbles, and avalanche chute margins (Fig. 5). On glaciers offset crevasses were measured, as well as matched faces on opposite sides of rhombohedral pull-aparts (Fig. 8A). These pull-aparts produced deep (perhaps >30 m) rhomboid chasms with parallel facing walls. However, we were unable to measure offsets on long stretches of the fault trace through glacier ice because of the complex nature of the trace and the web of small offset fractures radiating from the primary fault trace (e.g., Fig. 4B). For this reason, there are, and will remain, large gaps in the locations of measurements on the glaciers.

In measuring offsets, preference was given to sites that had relatively simple surface ruptures (one or a few traces in a zone 1- to 5-m across) and piercing points that could be confidently correlated across the fault (Fig. 4C,D). Even so, there is uncertainty in the measurements that primarily reflects uncertainty in the geometry of a feature prior to its offset. Few features are straight as they cross the fault trace. For example, does the curvature of a stream channel margin at the fault represent tectonic warping, or is it the initial channel shape? We inferred the curvature was related to faulting if ground cracking was coincident with the curve in the stream. Also, the original near-fault geometry of some features was obscured by deformation within the fault zone. To account for this the orientation of a piercing feature was projected to the fault from both sides of the offset, typically from a distance of 10 to 20 m. Each slip value is the measurement of the preferred geometric reconstruction of piercing point geometry and is not a statistical mean of multiple measurements (Fig. 9). For all the summer measurements, the positive and negative error values are the measurements at the maximum and minimum alternative projections. This was also done for some of the November measurements; for others a symmetrical error was estimated. Overall the error estimates are quite small. For the horizontal offset measurements shown on Figure 9, 59 (60%) have uncertainties that are less than 10% of the measured values, 25 (25%) have uncertainties that are 10–20% of the measured offset, 4 (4%) have uncertainties of 20–30%, 9 (9%) have uncertainties of 30–40%, and 2 (2%) have measurement uncertainties of 40–50%.

Characteristics of the Slip Distribution

The measurements of right-lateral offset along the entire Denali-Totschunda rupture are shown on Figure 9 and listed in Appendix 1. Because of the compressed aspect ratio of the slip-distribution plot (Fig. 9), the measurement uncer-

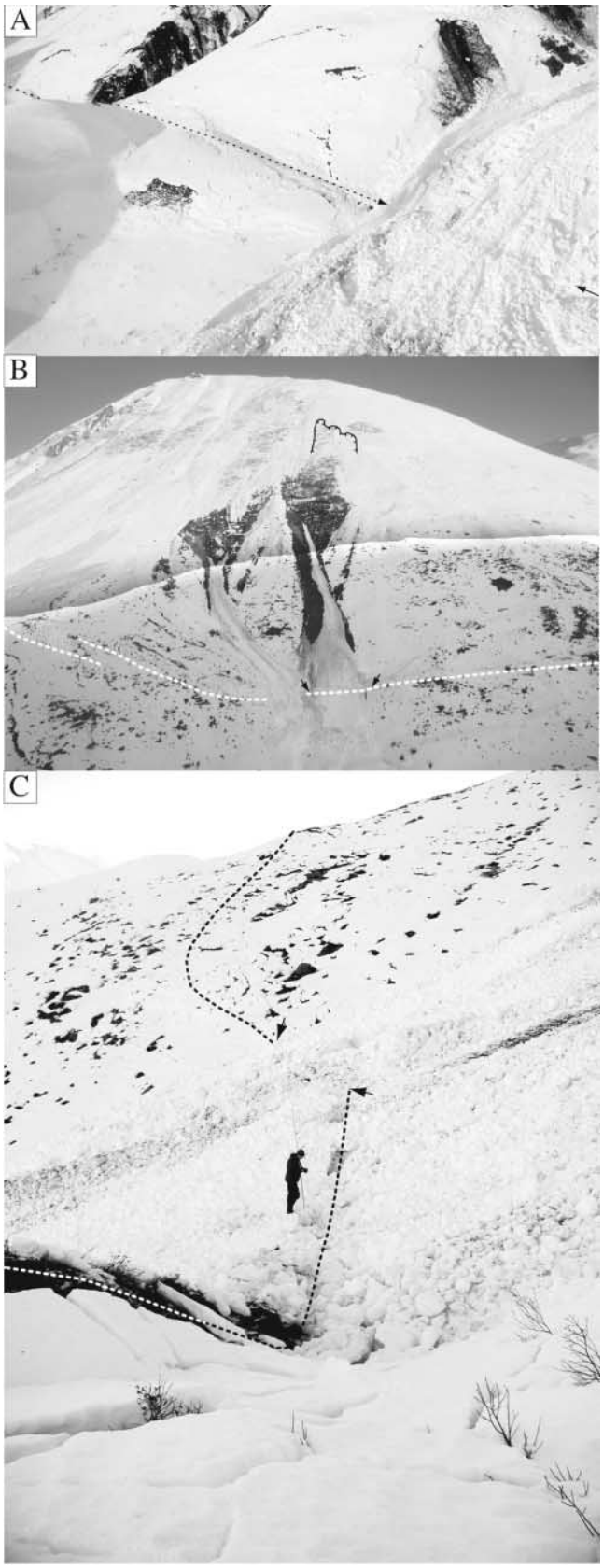

Figure 7. Relationships between snow avalanches and 2002 fault traces. (A) Typical snow avalanche whose debris covers the 2002 trace of the Denali fault (between arrows). Photograph view is to the north at about km 190. The fault trace, where, the fault scarp was covered by avalanche debris, is shown along the right side of the photograph between the arrows. Fault trace on left side of photo is shown along dashed line. Also note the numerous small slab avalanches exposing bare ground beneath the snow on the steeper slopes. These snow avalanches were very common adjacent to the surface trace. (B) Overview of only locality along any surface trace where snow avalanche debris is offset by the 2002 trace of the Denali fault. View is to the north at km 25.3. 2002 fault trace shown with white dashed line. Snow avalanche debris, between arrows, on right is offset by fault trace; snow avalanche debris on left, where there is a gap in the dashed line, is not. Headscarps of slab snow avalanches above chute is shown with the hatched line. Note the avalanche offset by the fault trace and the avalanche that covers the fault trace appear to be the same age. Photograph was taken when there was a very strong shadow, so this photograph was split in half and optimized for brightness and contrast in, or out of, the shadow. (C) View on ground of location shown in B. View is westward along fault trace, which is shown with white and black dashed line. Avalanche debris is offset in front of the person (2-m tall), but covered between the arrows.

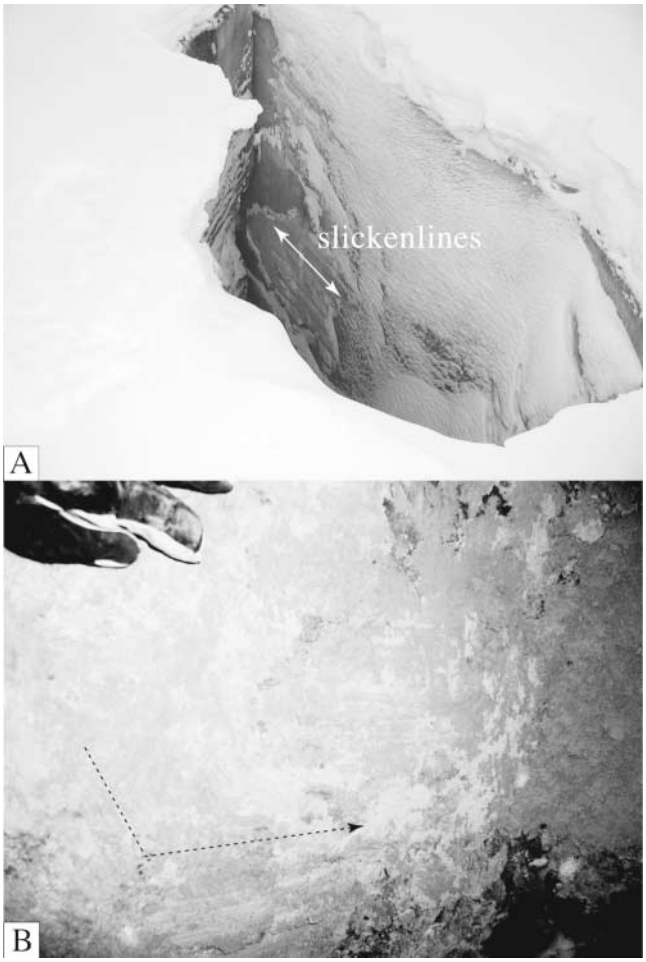

Figure 8. Photographs of slickensides at two locations along the surface trace. (A) View in a pull-apart in glacier ice on the Canwell Glacier at km 108.3 that shows a ~1.25 × 1.25-m square face on the ice in which horizontal grooves can be seen. This is also an excellent example of a rhombohedral pull-apart in glacier ice, where matching faces at the upper left and lower right show the offset to be 3.8 m. (B) This locality at km 239.0 is along the Totschunda fault and shows slickensides with a rake of 70° to the southeast, which turn abruptly to subhorizontal slickensides. Gloved fingers for scale.

tainties appear large relative to the preferred values. The vertical component of slip is shown on Figure 10.

The distribution of horizontal slip on the Denali and Totschunda faults is asymmetric (Fig. 9). Slip values rise from about 2 m near the west end to nearly 9 m just west of the intersection between the two faults. Slip on the Totschunda fault is no more than 3 m. Inspection of Figure 9 shows four distinct sections of the rupture within which slip values are relatively similar. These are (1) a low-slip (0–2 m) section from the epicenter to km 42, (2) a long section from km 42 to km 174 where slip is typically between 4 and 6 m, (3) a high-slip (6–8 m) section between km 174 and km 234 that contains the largest measured offset of 8.8 m, and (4) the Totschunda rupture between km 234 and km 302. Within each of these sections the offset measurements suggest there are additional shorter and distinct slip sections, which we discuss in a following section. In addition, field work in July 2003 and 2004 noted discontinuous fractures with little or no offset that extended 56 km from the epicenter westward along the unruptured (in 2002) western Denali fault.

km −56 to the Epicenter: Fractures West of the Epicenter. Mapping of fault ruptures in the epicentral region was complicated by deep snow cover in November 2002, small and intermittent displacements, the position of some scarps on very steep slopes, and a probable right step in the fault trace around km 17. A field party landed at two locations on this part of the fault in November, at 5.0 and 5.8 km west of the epicenter. They noted numerous displaced blocks of snow and fractures in the snowpack. However, there was no consistent orientation to the fractures, and it was concluded there was no surface offset.

In July 2003 and 2004, discontinuous fractures up to 20 m long were found superimposed on pre-existing Denali fault scarps in the region of both the 23 October and 2 November epicenters (Figs. 2B, 3I,J). Their locations are tabulated in Appendix 2. These fractures were first observed in July 2003 1.2 and 2.4 km west of the 3 November 2002 epicenter. They consisted of intermittent cracks, 5–10 m long, that had 1 to 3 cm of right-lateral offset (km −1.25) and less than 10 cm of south-side-down vertical displacement (km −2.36, Appendix 2). They occur along or adjacent to scarps produced by prior offsets. In all cases, the fractures are linear and occur in a variety of surficial deposits on gentle terrain with no evidence of mass movements.

During July 2004, additional fractures were observed and traced intermittently as far as 56 km west of the 3 November 2002 epicenter. Their length locally reached about 50 m (Fig. 3I). In general, these were found in wet areas, with sand blows at several locations, and in almost every case one side of the fracture moved 2–7 cm in the downslope direction. However, a few of these fractures occurred where there was little local topography (km −1.25). At km −35, the Denali fault trace and the fractures ran down a dry, gentle, broad west-facing slope and had 2–5 cm of right-lateral offset. There was no indication the fractures were related to mass wasting. It is unclear to what degree these fractures record incipient tectonic surface offset or a response to strong ground motion.

It is not certain which earthquake caused the fractures west of the November epicenter. The discontinuous fractures lie in the region near the 23 October foreshock and the 3 November mainshock epicenters (Fig. 2B). Aftershocks from the 23 October Nenana Mountain earthquake lie as far east as the 3 November epicenter, and extend about 70 km westward. On October 23, no cracks were observed on an overflight of the Denali fault in the epicentral region of the

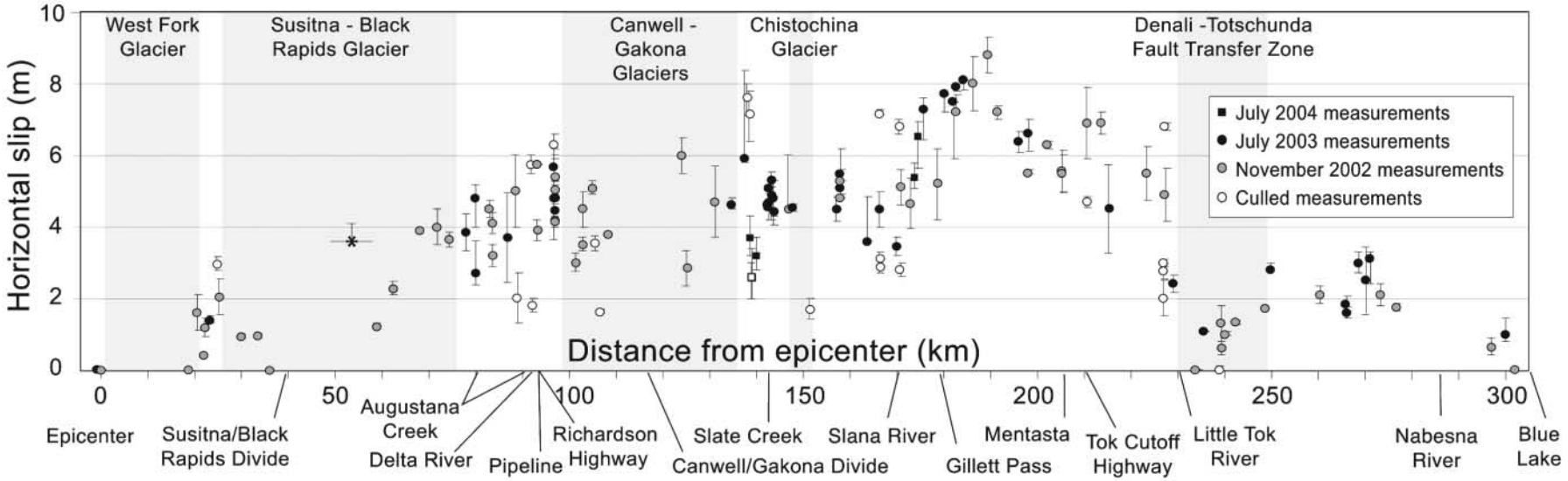

Figure 9. 2002 slip distribution along the Denali and Totschunda faults. Areas of glaciers and the transfer zone between the Denali and Totschunda faults are shown in gray. Data are listed in Appendix 1. Asterisk shows offset value determined by using GPS along Black Rapids Glacier by Hreinsdóttir (personal comm.). Horizontal bar shows region in which GPS stations lie.

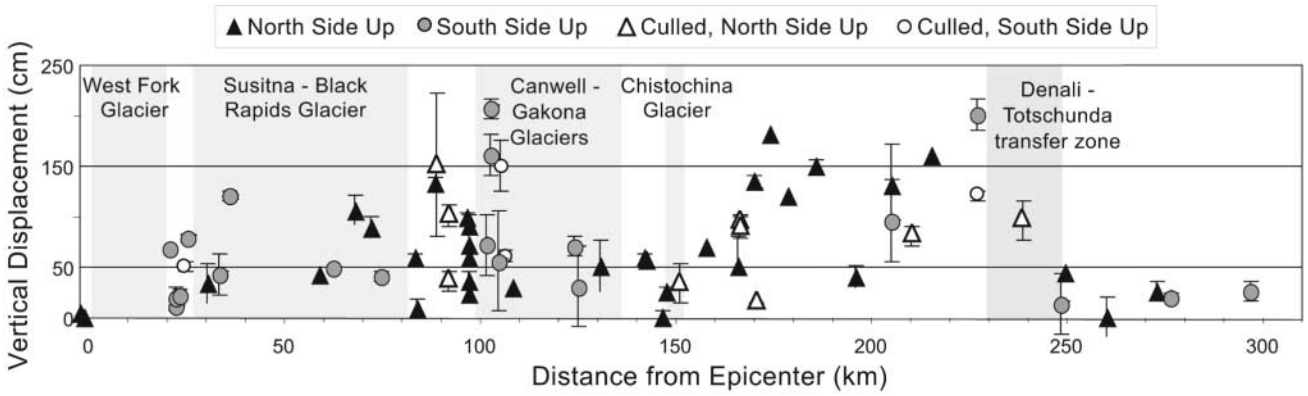

Figure 10. 2002 vertical slip distribution along the Denali and Totschunda faults. Note: one measurement is not shown because it is off scale. It is at km 239.15 with 2.7 m vertical slip.

Nenana Mountain earthquake. However, observation conditions were less than ideal, and snow cover may have obscured small-displacement discontinuous cracks. Thus, we are unable to ascribe their origin to a particular earthquake.

Epicenter to km 42: The Western End of Continuous Rupture. Fresh scarps of probable tectonic origin occur intermittently from 5 to 12 km east of the epicenter across three bedrock ridges along the north side of the West Fork glacier (Fig. 2), and we informally refer to these as the West Fork ruptures. These scarps were first seen during July 2003. They could not be reached on the ground because of extremely steep terrain, but they were observed at relatively close range by helicopter. At that time, there was no observed fracturing on the West Fork Glacier between the ridges nor between the westernmost ridge and the epicentral region. These nearly continuous ruptures strike east-northeast (074°) along steep, south-facing, rubble-covered bedrock slopes, and in talus-filled gullies between bedrock ridges. Right-lateral offsets of gully margins of as much as 1 to 2 m and north-side-up scarp heights of 1 to 2 m were estimated from the air. Because the amount of offset could not be directly measured, these estimates are not included with the slip data table (Appendix 1). After considering these uncertainties, we use 1 m as an estimate of right slip for this short section of the rupture.

It is uncertain whether the West Fork ruptures are located on the main trace of the Denali fault. They do not appear to lie on pre-existing scarps and are located up to 4 km north of the mapped trace. At about km 17 the rupture appears to step southward and right about 4 km to the more easterly striking (094°) continuous rupture in the Susitna drainage (Fig. 2). If this is the main trace of the Denali fault, there is a 4-km right step, the largest of the 2002 rupture. Alternatively, this could be a splay with the main trace beneath the West Fork Glacier.

The westernmost continuous rupture, which was noted in November 2002, starts at km 18.75. The slip rises sharply from values near zero meters to 1.2 to 2.0 m between km 20.5 and km 25.3 where the rupture is observed on land. The location and rate of increase in slip to the east is uncertain where the surface rupture traversed the Susitna and Black Rapids Glaciers. The combination of a sometimes broad and complex rupture pattern across these glaciers (Figs. 4, 6) and landslide debris that buried the fault trace along much of the Black Rapids Glacier limited the number of offset measurements. Only three measurements, with none larger than 1 m, were made between km 25.3 and km 50. Hreinsdóttir (personal comm., 2004) used GPS to remeasure locations of benchmarks along the margins of the Black Rapids Glacier between km 49 and km 58. She found that a simple dislocation model demands a minimum of 3.6 m of right-lateral offset and, if there is some fault dip, right slip was as high as 4.1 m. It is uncertain where the eastward slip increase occurs. We chose km 42, because it is the midpoint between our measurement at km 36 and Hreinsdóttir's measurements beginning at km 49, but it could occur further west.

km 42 to km 174: The 5-Meter Section. From km 42 to 174 the majority of offsets are 4 to 6 m, though in detail shorter sections of the rupture appear to have distinctly different amounts of slip (Fig. 9). The 1.2-m and 2.3-m offsets we measured in glacier ice at km 59.0 and km 62.5, respectively, appear to significantly underestimate the total slip, as indicated by the GPS measurements of Hreinsdóttir (personal comm.), and they were culled. Offsets at the eastern end of the Black Rapids Glacier are about 4 m. Similar values are measured on land along nearby Augustana Creek and eastward to the Delta River (km 78–92). In all, eleven measurements between km 68.5 and km 88.5 range between 3.2 and 5.0 m with the majority between 3.6 and 4.8 m.

From near the Delta River (km 91.9) eastward across the Trans-Alaska Pipeline (TAPS, km 93.2) to at least near the toe of the Canwell Glacier (km 96.6) offsets of 5.7 to 5.8 m were measured (Fig. 9). Two TAPS high-resolution

GPS and photogrammetric surveys show 5.8 m of right slip across a 1000-m-wide zone at the pipeline. Of this total, 5.3 m of slip occurred within 100 m of the surface rupture and 1.3 m of offset at the main rupture trace (M. Metz, oral comm., Alyeska Pipeline Service Co., 2004). At km 96.3, a well-constrained slip value of essentially the same amount, 5.7 m, was measured on an offset channel margin across a narrow (2-m-wide) mole track. Between here and the west end of Canwell Glacier several well-developed small gullies in glacial outwash are offset 4.2–5.4 m. These are somewhat smaller than the highs immediately to the west and could reflect minimum values because the rupture here is stepping to the north.

Offsets between the toe of Canwell Glacier (km 97) and the eastern Slana River valley (km 173) are typically about 5 m (Fig. 9). Along much of this section the rupture occurs in glacier ice, including a 39-km length on the Canwell-Gakona Glaciers and 5 km on the Chistochina Glacier. On the Canwell and Gakona Glaciers nine slip values were made on offset crevasses and matching faces across extensional rhombohedra. A series of low values (2.85–3.55 m) were measured between km 101.5 and km 125.32. Although we do not consider the offset measurements in glacier ice to be as robust as those on land, five of these glacier measurements are between 4.5 and 6.0 m and are similar to values from adjacent on land sections. Because of this similarity we conclude that the larger offsets are representative of the slip in this area.

A series of excellent measurements, primarily on offset small gullies of intermittent streams and the margins of broader channels, were made in the Slate Creek and Slana River areas where the rupture is a commonly confined to a 2- to 4-m-wide mole track (Fig. 3G). This section ends before km 175.7 where the offset is 7.3 m. The distance over which this increase in slip occurs may be as little as 0.4 km, because a measurement of 5.4 m was made at km 173.8 and a higher measurement of 6.5 m was made at km 174.2. The rise to the higher slip values of the next section to the east is abrupt.

km 174 to km 226: The High Slip Section. The largest 2002 offsets occur along a 54 km-long section of the rupture between Gillett Pass and the Little Tok River (km 174 to km 228). Individual measurements range from 4.9 to 8.8 m with the majority larger than 6 m. Where these large offsets occur across south-flowing drainages the resulting upslope-facing scarps often completely block the active channels. Locally, the fault trace is very narrow and some of the 8-m offsets occur across a rupture zone only 1 m wide (Fig. 5E,G). Along this part of the fault we recognize two distinct slip sections. The first is an 11-km-long section with slip values larger than 7.0 m. It contains the maximum offset measured on the 2002 rupture, which is 8.8 m at km 189.4. The second has smaller offsets of 5–7 m and extends east of the maximum slip values to about km 226.

km 226 to km 250: The Transfer Zone. At km 234 the surface rupture turns southeast onto the Totschunda fault and the amount of offset drops dramatically. The rupture passes through the complex transfer zone (Fig. 6D) and onto the simpler single-strand section of the Totschunda fault at km 250. The transfer zone includes the easternmost 8 km of rupture along the Denali fault. The western limit of the zone is marked by rupture along a subparallel 1-km-long strand located about 0.5 km south of the main Denali fault trace at km 226 (Fig. 6D).

The transfer zone has northwest-striking strike-slip fault segments and northerly-striking normal fault segments that intersect at high angles (Figs. 2, 6D). A 4.9-m offset at km 227.2 is the easternmost large slip value measured along the Denali fault. Only 1.8 km to the east (km 229.0) the horizontal offset decreases to 2.4 m and then drops to about 1 m across the extent of the zone. At the easternmost rupture along the Denali fault (km 229.0) deformation spans a zone more than 45 m wide. This broad deformation indicates that, at least locally, we may not have measured the total horizontal slip in parts of the transfer zone.

Three vertical slip values of about 2.0–2.7 m were measured on the normal fault segments. The large vertical slip components are consistent with the right (transtensional) bend between the Denali and Totschunda faults. The intersections between normal and strike-slip fault segments are locally very distinct, occur over lateral distances of as short as 10 m, and have changes in strike between 25° and 85°.

Toward the southeast end of the transfer zone rupture occurred on two splays. The northeastern splay is the primary fault strand and has offsets of 1.0–1.7 m. The southwestern splay is 7.9 km long and slip at its northwestern end was measured at a few tens of centimeters. We consider the eastern limit of the transfer zone to be the point where the splays join at about km 250.

km 250 to 302: Continuous Totschunda Fault Rupture. Two segments of the Totschunda fault ruptured during the 2002 earthquake. The northeastern Totschunda Creek segment is ~49 km long, and the slip distribution appears to have a symmetrical shape (Fig. 9). Offset values lie between 1.6 and 3.1 m. Our November 2002 measurements indicated a maximum offset of about 2.0 m (Eberhart-Phillips *et al.*, 2003) but additional measurements in July 2003 show as much as 3.1 m (km 271). About 14.5 km of surface rupture occurred along the Cooper Pass segment (Fig. 2A) at the southeastern end of the 2002 surface rupture. The two offset measurements along this part the rupture are 0.6 and 1.0 m and are distinctly lower than the Totschunda Creek segment. There is a 4.2-km-long region at about km 289 with no surface rupture between the fault segments (Fig. 2).

Vertical Displacements. Measurements of vertical displacement range from 0 to 2.7 m and average 0.7 m (Fig. 10, Appendix 1). Along the Denali fault, vertical slip was

dominantly north-side-up (Fig. 10). This sense of slip is consistent at most on-land locations, particularly between the Black Rapids and Canwell Glaciers and for 90 km between the eastern edge of the Gakona Glacier and the Denali-Totschunda transfer zone. The only exceptions are at the westernmost end of the continuous surface rupture (km 20.5 to km 25.3) and east of Mentasta (km 202 to 205) where the rupture was south side up (0.1 m and 0.7 m, respectively). The sense of vertical slip on the glaciers is more variable and both north- and south-side-up displacements were observed. The Totschunda fault rupture has both northeast- and southwest-side-up scarps. Of the 11 locations measured here, four have no vertical component and the remainder have no preferred sense of vertical displacement.

Vertical slip generally increases with horizontal offset (Fig. 11), but there is large scatter in the data. A trendline through all Denali fault (nontransfer zone) data points shows that vertical slip is positively correlated at 17.7% of the horizontal. Eliminating glacier ice values, which may have been influenced by the ice fabric, does not significantly change the result (vertical = 17.3% of the horizontal). Along the Denali fault the largest vertical slip values are consistently 43% of horizontal slip values. The only exceptions are three data points from the transfer zone, where vertical slip is greater than horizontal, and one data point in glacier ice (km 102.9), where vertical offset was large. There was at least some vertical displacement for all points where the horizontal slip exceeded 4.5 m.

Discussion of Slip Distribution

The field observations of surface rupture and the distribution of horizontal and vertical surface slip are baseline data for understanding the Denali fault earthquake, the longer term behavior of the Denali fault, and long ruptures on strike-slip faults in general. In the following sections we discuss this data set and compare our observations with geodetic and seismologic models of slip and moment release for the event.

Has All the Slip Been Measured?

The use and interpretation of surface offset measurements for the Denali fault earthquake depend on the degree to which these capture the total coseismic displacement at the surface. In measuring offset across strike-slip ruptures, the question arises as to how much slip occurs in the near field of the main rupture zone and how much slip is distrib-

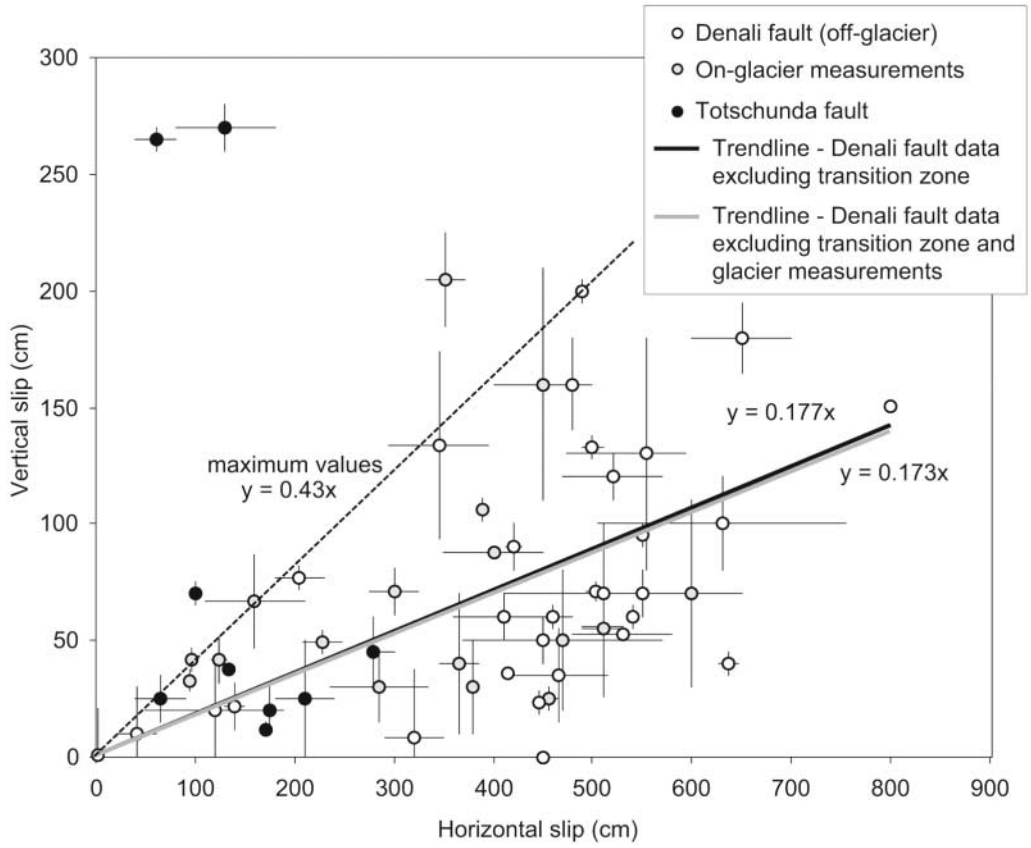

Figure 11. Plot of vertical versus horizontal slip along the Denali and Totschunda faults, and trendlines fit through the data. R^2 value of preferred trendline for Denali fault off-glacier and non-transfer-zone data is 0.28. Data from Appendix 1.

uted tens to hundreds of meters away from the fault. Offset measurements on man-made features, where the geometry is known, are ideal for observing the way in which slip is distributed across a fault zone. Observations of historical strike-slip ruptures show there can be a range of deformational effects on cultural features, such as roads, fences, and tree lines (e.g., Lawson, 1908; Rockwell *et al.*, 2002). These include (1) complete slip across a narrow surface rupture; (2) a high percentage of slip across the brittle rupture accompanied by a small amount of slip in an adjacent 5- to 10-m-wide zone of warping; (3) slip distributed across broad zones of en echelon or parallel ruptures, particularly at bends or steps in the fault trace; and (4) broadly distributed slip in areas of saturated deposits.

Along the Denali fault rupture only three fault crossings with man-made features provide long baselines. These are the Trans-Alaska Pipeline, the adjacent Richardson Highway, and the Tok Cutoff Highway (Fig. 2A). A high-resolution survey along the TAPS (M. Metz, Alyeska Pipeline Service Co., written comm., 2004) measured a total of 5.8 m right-lateral slip and 1.3 m of north-side-up displacement distributed across 1000 m. Within this zone, 4.9 m (84%) of the offset occurred in a 100-m-wide zone straddling the surface trace. The two closest survey points on either side of the fault trace are about 25 m apart and measured 3.3 m (57%) of right-lateral offset. Offset at the fault trace itself was 1.3 m. On the adjacent Richardson Highway, measurements made 7 days after the earthquake showed lateral slip of 3.9 m across a 75-m-wide zone; 3.4 m of this occurred across the primary fault trace. A nearby borehole encountered ~240 m of unconsolidated Quaternary sediments (M. Metz, personal comm., 2004). At the Tok Cutoff Highway, there was 5.0 m of offset distributed across a 20-m-wide zone containing two fault strands and adjacent zones of warping (Fig. 5D). There was an additional 1.9 m of offset in a zone 500 m north of the fault.

The geologic settings of the TAPS and the adjacent Richardson Highway are atypical of the surficial conditions along much of the 2002 Denali fault rupture. The TAPS and Richardson Highway are on a thick sequence of young saturated fluvial deposits of the Delta River. The pre-2002 fault scarp could not be identified or directly traced across the pipeline route during preconstruction studies (Woodward-Lundgren Associates, 1974) and was projected across the proposed route from known locations. In contrast, the pre-existing scarps along most of the Denali fault are obvious and easily mapped. This suggests that either a structural complication or, more likely, that near-surface geologic conditions caused broadly distributed deformation. Where the Denali fault cuts the Tok Cutoff Highway, Quaternary valley-fill sediments are water saturated, as indicated by numerous bogs and small ponds. It appears that thick, water-saturated sediments produced distributed deformation.

Most of our measurements were made where the fault is a single trace (or closely spaced traces), the width of the rupture zone is narrow, there is clear geomorphic expression of previous rupture, and there is an absence of thick, water-saturated fill. Any single location, if measured in isolation, does not provide the perspective for evaluating whether surface slip has been underestimated or overestimated. However, we have multiple measurements along sections of the surface rupture that are tens of kilometers long and characterized by similar slip values. For example, along the 79-km-long section between km 96 and km 173 where offsets are commonly around 5 m, twenty-three offsets (and their uncertainties) center near 5 m, five are below 4 m (four of these are glacier measurements, see below), and one is at or above 6 m. Similar observations can be made along other sections of the rupture. From this we infer that our measurements capture essentially all the coseismic surface slip.

The Slip Distribution: Variability and Average Slip

The measurements of surface slip along the Denali and Totschunda faults show variation at two scales. The first is point-to-point, or high-frequency, variability. Plots of surface slip from historical ruptures on all fault types commonly show spikes in values of closely spaced measurements (Crone and Machette, 1984; McGill and Rubin, 1999; Rockwell *et al.*, 2002; Treiman *et al.*, 2002). The Denali fault data set is no exception, containing some measurements that fall well below, or in some cases well above, the values at adjacent points even though the uncertainty in an individual measurement is small. Changes in slip values as large as 1.5 m (although still within the uncertainty range of neighboring points) occur in short distances, such as near the west end of the Canwell Glacier (km 96.63 to km 97.0), Slate Creek (km 142.14 to km 143.75), and east of Chistochina Glacier (km 157.1 to km 157.72) (Fig. 9). Apart from localized structural complications, it is not clear why this high-frequency variability occurs. It could reflect a combination of measurement error, incomplete expression of slip at the surface, or actual short-distance variability in the coseismic surface slip.

Broad wavelength variation in slip also occurs. As noted and described previously, there are four distinct slip sections on the strike-slip faults between the epicenter and the east end of the rupture. These have typical offsets of 0 to 2 m (epicenter to km 42), 4 to 6 m (km 42 to km 174), 6 m to almost 9 m (km 174 to km 228), and 1 to 3 m (km 228 to km 302). The measurements also suggest that these can be subdivided into additional slip sections and slip steps. The broad wavelength slip variation, in contrast to point-to-point variability, provides important insights into the 2002 rupture process.

Average Slip from Surface Measurements

The average slip and the location and rate of change of slip along strike provide a basis to calculate seismic moment for the 2002 earthquake from surface-rupture parameters. The slip distribution can also be used for comparison with

geodetic and seismologic models of slip distribution and strong-motion estimates of moment release. To calculate average slip, the surface measurements must be averaged over some length of the fault trace. For the rupture as a whole, we recognize a total of 10 slip sections, with internally consistent, but distinctly different, amounts of slip (Fig. 12)

We use three methods to do this: (1) a 5-km running average using all the data points (and excluding culled points); (2) an envelope of maximum slip values; and (3) a graphical approach. For each, we derive the average slip for the distinct rupture sections described previously (Fig. 12). For the running average and envelope of maximum slip the curves are drawn through the preferred (central) slip value at each measurement point.

A running average of all data points is shown on Figure 12A. We use a 5-km running average of the data points at each kilometer along the rupture. In doing so, several data points are usually included in the average (Fig. 12). A 10-km running average results in too much smoothing of the slip distribution; a narrower interval would not average multiple data points based on the present distribution of measurements. Where there are no observations within a 5-km-length a running average cannot be calculated and the running average line segments are connected with dashed lines that may approximate the slip distribution. Slip is then averaged for each of the distinct fault sections. From west to east these values are 0.7, 1.3, 3.7, 4.8, 4.5, 7.2, and 5.7 m on the Denali fault and 1.5, 2.0, and 0.7 m on the Totschunda fault. The running average is the least interpretive of the methods because it weights each data point equally. This may lower the average slip values along some sections of the rupture. For example, the running average curve decreases sharply in the western part of Canwell Glacier because it incorporates low glacier values that likely underrepresent the actual slip in this area. The 5-km running average yields an average slip of 4.4 m on the Denali fault and 1.6 m on the Totschunda fault, and a combined average slip of 3.7 m for the strike-slip rupture.

The slip distribution drawn through the maximum horizontal offsets defines an envelope of maximum slip (Fig. 12B). This envelope yields the largest value of average slip for the 2002 rupture. For each of the ten slip sections, we averaged the slip along the maximum envelope at 2-km intervals. From west to east these averages are 0.8, 2.2, 4.0, 5.6, 5.4, 7.7, and 6.2 m on the Denali fault, and 1.8, 2.1, and 0.8 m along the Totschunda fault. The average maximum horizontal offset is 5.0 m on the Denali fault, and the average for the Totschunda fault is 1.7 m. The combined average along the entire surface rupture is 4.2 m. We believe these values place a realistic cap on the average maximum horizontal slip along the 2002 strike-slip surface rupture.

The slip averaged for sections of the rupture by using a graphical method is shown on Figure 12C. For each slip section, we visually fit a horizontal line to include as many of the representative offset values and their uncertainties as possible. This method is subjective, but its strength is that judgment can be used to favor certain data points, such as the pipeline surveys. The resulting average slip values are 1.0, 1.5, 4.1, 5.8, 5.0, 7.8, and 6.1 m on the Denali fault and 1.2, 2.5, and 0.8 m on the Totschunda fault. The average horizontal offset for the Denali and Totschunda faults is 4.8 and 1.8 m, respectively. The average for both faults is 4.1 m.

To calculate the net average slip, the vertical component must be included. As discussed previously, the consistent up-to-the-north vertical displacements along the Denali fault are correlated with the horizontal slip at 0.173 (Fig. 11). The lack of a consistent sense of vertical slip along the Totschunda surface rupture indicates that an additional vertical component should not be added for this fault.

Including the vertical component of slip yields a net slip vector that is larger than the average horizontal slip. It would be ideal to measure net slip vectors in the field, which could have been readily done if the slip had been confined to a single rupture surface. However, the presence of ubiquitous local structural complications and typical fault zone widths of 1–4 m made it difficult to do this reliably or consistently. Therefore, we use the general relationship between horizontal and vertical slip along the Denali fault shown on Figure 11. Using the slip calculated for each of the three averaging methods with an additional 17.3% factor for the vertical component yields an average net Denali fault slip of 4.5 m for the 5-km running average, 5.1 m for the maximum slip envelope, and 4.9 m for the graphical method. These are the range of values we use to calculate the earthquake's moment magnitude from the surface fault parameters.

Slip Steps: Steep or Gradual?

We identify ten sections of the surface rupture, seven on the Denali fault and three on the Totschunda fault (Fig. 12). These sections range in length from as short as 10 km to as long as about 90 km. In Table 2, we summarize the changes in the amount of slip (increases and decreases) that occurred between six of the better constrained slip sections of the Denali fault and the maximum distance over which they occurred. Five of the six slip steps are distinct; the small decrease interpreted east of km 97 is less certain, largely because of uncertainties in the amount of slip through the Canwell Glacier. The step near km 228 is within the Denali-Totschunda transfer zone, and because deformation may be more distributed the step may not be as large as indicated on Figure 12. Nonetheless, there is clearly a large decrease in slip between the Denali and Totschunda faults. The difference in the amount of slip across the four sections is calculated by using the 5-km running average, the average maximum envelope, and the graphical methods. Regardless of method used, the results are similar. The largest increase is in the Slana River Valley west of Gillett Pass (km 173.0–175.7). A distinct increase of 1.1 to 1.7 m is just west of the TAPS (km 88.5–93.2). Decreases also occur west of Mentasta (km 191.5–195.9) and just west of the Little Tok River (km 227.2–229.0). The two segments of the Totschunda

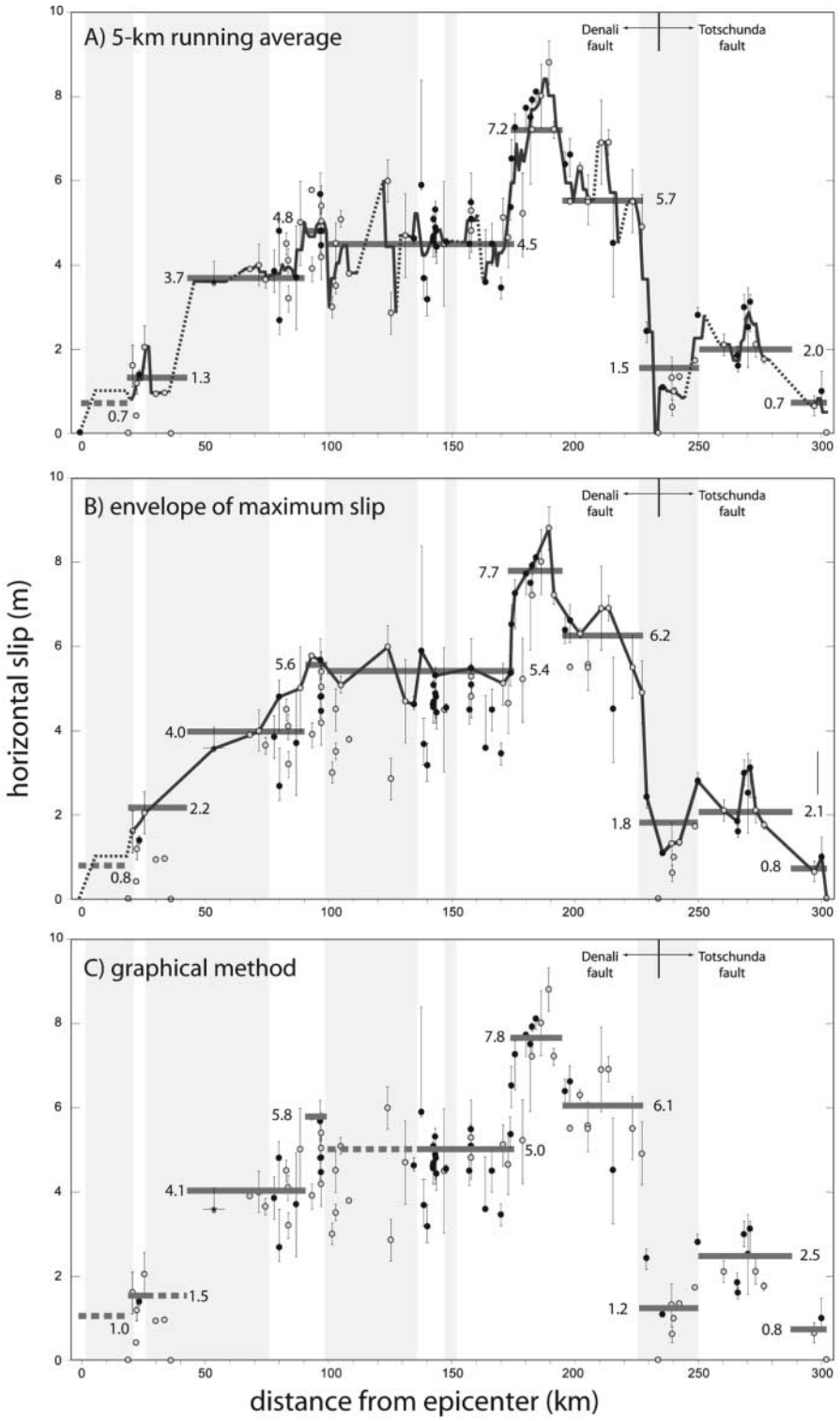

Figure 12. Estimates of average slip distribution from three methods. For all figures, the symbols for the data are the same as in Figure 9. The vertical gray bars show the regions of rupture through glacier ice. The vertical gray bar at the Denali and Totschunda fault junction shows the region of the transfer zone between the faults. Segments with similar slip, as discussed in the text, are shown with horizontal gray bars. The number adjacent to the bars gives the value in meters for the segment. The westernmost bar in all three diagrams is dashed because offset was estimated from the air, as discussed in the text. (A) 5-km running average of all data points. The average is dashed for regions where data points are lacking. (B) Envelope of maximum slip values. (C) Graphical method.

Table 2
Location and Size of Slip Steps Along the Denali Fault

Distance East of Epicenter (km)	Maximum Distance across Step (km)	Change (±): Running Average (m)	Change (±): Average Maximum (m)	Change (±): Graphical Method (m)
88.5–93.2	4.7	1.1	1.6	1.7
97.0–101.5	3.1	−0.3	−0.2	−0.8
173.0–175.7	2.7	2.7	2.3	2.8
191.5–195.9	4.4	−1.5	−1.5	−1.7

fault have distinct slip values, but there are not enough observations near the transition between the strands to clearly define the gradient between them.

There is some evidence that changes in slip along the fault can be abrupt. The distances listed in Table 2 are between the closest measurements on either side of a step and they define the maximum distance over which the slip change has occurred. Because there are gaps between measurements it is not known if the slip changes occur over hundreds of meters or gradually over the entire distance. The best evidence for a rapid change in slip is between the 5-m and the high-slip sections. Kilometer 173.8 is the easternmost point along the section where offsets are about 5 m, and by km 174.2 the measured slip is 6.5 m. At km 175.7 the measured slip is 7.3 m.

Earthquake Moment Magnitude from Surface Fault Parameters

The moment magnitude, M_w, can be calculated from observed fault parameters (Table 3). The seismic moment, M_o, of an earthquake is the product of fault area (rupture length and width), average slip, and shear modulus (assumed to be 3×10^{11}). This can be converted to a moment magnitude, M_w, by the relation $M_w = 2/3 \log M_o - 10.7$ (Hanks and Kanamori, 1979). To calculate M_w for the 2002 Denali fault earthquake, we use the fault lengths listed in Table 1 and summarized in Table 3. The thickness of the seismogenic crust, or locking depth, is considered to be 12 km based on the maximum depth of aftershocks (Ratchkovski *et al.*, 2003). Aftershock depths are well constrained only along the Richardson Highway, but it is reasonable to assume a similar depth for the entirety of the rupture. This gives the width of the vertical strike-slip faults. For average slip, we use the 5-km running average values, the envelope of maximum slip values, and the graphical method values discussed previously with an additional vertical component for the Denali fault. For the Susitna Glacier fault, we use a 17-km down-dip width, calculated from the thickness of the seismogenic crust and a fault dip of 40° based on the focal mechanism. We use a fault length of 40 km, which is the length of the chord between the end points of the surface rupture and an average slip of 4.0 m (Crone *et al.*, 2004). The length we use is slightly shorter than that used by Crone *et al.* (2004), because we consider it unlikely that the average slip occurred over the entire 48-km length of the fault. Nonetheless, the resulting moment and moment magnitude are essentially the same.

The seismic moment and moment magnitude of the earthquake can be derived from summing the moments of each fault. Using the three averaging techniques for average slip gives $M_o = 4.84–5.40 \times 10^{27}$ and $M_w = 7.79–7.82$. The fact that one qualitative and two quantitative techniques for averaging slip-distribution data yield the same moment magnitude demonstrates the result is robust. The calculated moment magnitude is insensitive to small changes in rupture length, width, or average slip. Given that the seismologically derived moment magnitude is qualitatively accurate to ±0.1 (A. D. Frankel, written comm., 2004), our geologically derived M_w 7.8 is in very good agreement with the **M** 7.9 determined from strong-motion seismology.

There are several ways to calculate a slightly larger moment magnitude than the calculated M_w 7.8 by modifying of fault parameters: (1) increasing the width of the fault zone, (2) increasing the slip at depth, or (3) increasing the shear modulus. We only discuss changes in parameters to the Denali fault, because it has about five and ten times more moment release than the Susitna Glacier and Totschunda faults, respectively (Table 3). First, the down-dip width of the fault zone could be more than 12 km, which would imply that aftershocks did not occur in the deeper parts of the primary rupture zone. A moment magnitude of 7.9 can be calculated if the width of the entire Denali fault zone is increased from 12 to 18 km. Second, the slip at depth could be greater than the slip measured at the surface (Ji *et al.*, 2002). If the Denali fault average slip is increased from our values of 4.46–5.08 m to 7.4 m, an M_w 7.9 is calculated. Third, the shear modulus is commonly assumed to be 3.0×10^{11} for average "crustal" rocks, but some of the rocks along the Denali fault trace are mafic, and thus a higher modulus may be appropriate. A shear modulus of 4.5×10^{11} would be required to calculate an M_w 7.9.

It is unlikely that any of the actual fault parameters are as different as those required to calculate a moment magnitude of 7.9. To increase the width of the seismogenic zone to 18 km is a 50% increase, which is inconsistent with the observed seismicity and current geodetic models. To increase the average slip to 7.40 m from our average values of 4.46 to 5.08 m (including the vertical slip component) is an increase of 50–64%. For reasons discussed earlier, we do not think we are missing much slip in our observations. Although slip is commonly inferred to be locally greater at depth than at the surface along strike-slip ruptures, it seems improbable that slip would be greater at depth for the entire length of the rupture. Last, a shear modulus of 4.5×10^{11} is 50% higher than typical values, which also seems unlikely based on consideration of crustal seismic velocities (Brocher *et al.*, 2004).

Comparison of Geologic Slip Distribution with Geodetic and Seismologic Slip Models

The preceding sections presented the geologic observations on the strike-slip surface faulting associated with the 2002 Denali fault earthquake. A variety of seismologic and geodetic models of the rupture process, slip distribution, and moment release have been proposed. Here, we compare these with our direct observations of slip.

Strong-Motion Model

Frankel (2004) inverted the strong-motion data to determine moment release along 3-km-long segments of the Denali and Totschunda faults (Fig. 13). The inversion yields moment averaged over the upper 10 km of faulting depth. The large-scale features of the strong-motion inversion are seen in the geologic slip distribution. The strong-motion inversion has low moment release along the fault from 0 to about 85 km, moderate moment release from 85 to 175 km, high moment release from 175 to 230 km, and low moment release from km 230 to the end of the rupture. These amounts of moment release and their locations along the faults correlates well with the observed surface slip. Two major subevents in the strong-motion inversion correlate with our slip steps (Table 2). A pulse of moment release east of the TAPS (km 93.2) correlates with a surface slip step in the same region. The onset of the largest pulse of moment release coincides with a surface slip step of 2.2–2.8 m between km 173.0 and 175.7 (Table 2)

Table 3
Parameters for Calculation of M_o and M_w

			Average Net Slip (cm)			$M_o \times 10^{26}$ (dyne cm^2)			
Fault	Rupture Length (km)	Width (km)	5-km Running Average	Envelope of Maximum Slip	Graphical Method	5-km Running Average	Envelope of Maximum Slip	Graphical Method	M_w
Denali	226	12	446*	508*	487*	36.3	41.4	39.6	7.7
Totschunda	66	12	156	171	184	4.0	4.4	4.8	7.1
Susitna Glacier	40	17	400†	400†	400†	8.2	8.2	8.2	7.3
Total						48.5	54.0	52.6	7.8

*Includes a 17.3% vertical component as discussed in the text.
†Susitna Glacier fault slip is that calculated by Crone *et al.* (2004).

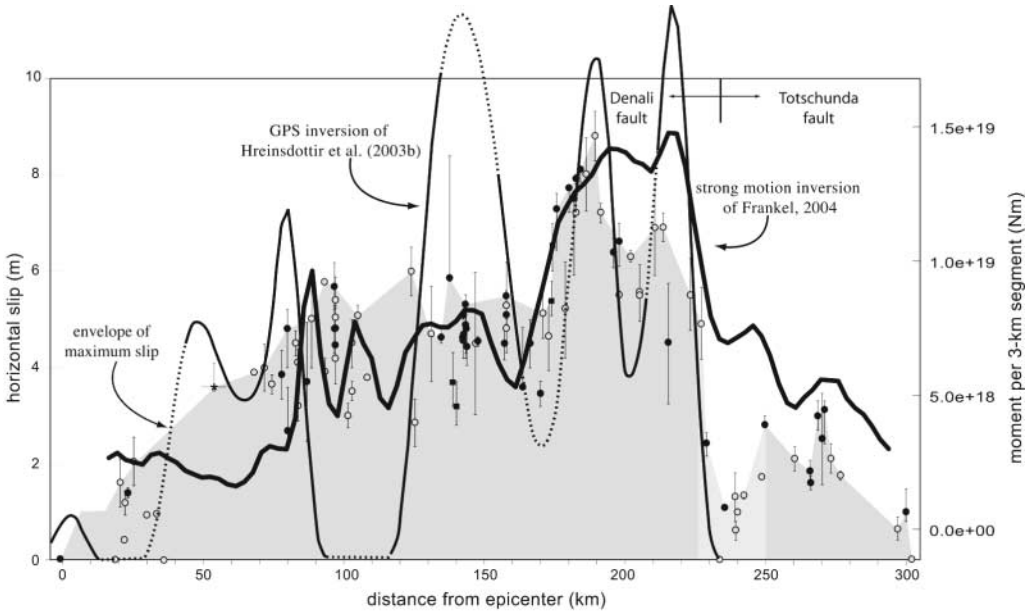

Figure 13. Comparison of surface slip distribution (from envelope of maximum slip) to strong-motion and geodetic models of moment release along the Denali and Totschunda faults. Thick black line shows the strong-motion inversion of Frankel (2004). Thin black line shows the GPS geodetic inversion of Hreinsdóttir *et al.* (2003b); dashed line shows where the inversion is poorly constrained. Vertical scale for strong-motion inversion of Frankel (2004) is shown on the right. Symbols are the same as in Figure 9.

The general colocation of strong-motion subevents and changes in the amount of surface slip has important implications. Systematic geologic investigations can map the distribution of surface slip for preinstrumental and prehistoric earthquakes along strike-slip faults. For example, Sieh (1977) developed a slip distribution for the 1857 Fort Tejon earthquake that showed broad wavelength variations and slip steps similar to our Denali-Totschunda slip distribution. Therefore, it may be possible to use the locations of slip steps to improve predictions of strong ground motion for future large earthquakes.

Geodetic Model

Hreinsdóttir *et al.* (2003b) inverted GPS data to model coseismic slip (Fig. 13). Their model shows the same large-scale pattern as the geologic observations, with slip increasing from west to east. However, in detail their results do not correlate well with the surface observations. Hreinsdóttir *et al.* (2003b) also identified sections of the rupture where geodetic model resolution was poor. For the well-resolved areas, the geodetic model and geologic observations are quite consistent west of km 90. However, between km 185 and the end of the Denali fault rupture at km 234, modeled geodetic slip is nearly double the observed maximum surface slip (Fig. 13). For the poorly resolved sections little or no surface slip is modeled east of the TAPS for about 40 km, and as much as 10 to 11 m is shown between about km 135 and 155. The maximum average right-lateral surface offset along this entire reach of the fault is 5.4 m. The poorly resolved section between km 155 and km 180 indicates surface slip as small as 2 m, but at this location the surface slip is increasing toward the largest offsets. The geodetic model does not constrain slip on the Totschunda fault southeast of the transfer zone.

Teleseismic Model

Broadband teleseismic records are commonly inverted to model the source processes of earthquakes. Kikuchi and Yamanaka (2002) used waveforms to model the 2002 event. They correctly concluded that the rupture was a sequence of subevents with the first occurring on a reverse fault that turned out to be the Susitna Glacier thrust. Their slip distribution shows the amount of offset increasing eastward. The region of largest slip in their model, at about km 140 to km 180, coincides at its eastern end with the largest surface offsets. However, it estimates the maximum slip at 12 m, in contrast to the 8.8 m we measured, and it underestimates the rupture length by some 50 km.

Implications

The surface slip distribution from the 2002 Denali fault earthquake can be used to test and constrain geophysical models of the rupture. These models should reproduce or yield a pattern of slip or moment release very close to the measured surface offset. One of the most intriguing observations is the apparent relation between distinct changes in the amount of surface slip and the occurrence of strong-motion subevents and large accelerations. An important goal of paleoseismic studies is the collection of information on the amount and distribution of slip in past earthquakes. Paleo-offset data can be used to estimate the magnitude of paleoevents, and changes in the amount of slip along strike could provide a basis for improving the modeling of strong ground motion in future earthquakes.

Conclusions

Great strike-slip earthquakes, produced by faulting that extends for several hundred kilometers in shallow crust, are not common. Since 1900 they have typically been in remote areas such as China (1920, Haiyuan fault), Turkey (1939, central North Anatolia fault), Mongolia (1905 Bulnay fault; 1957 Bogd, Toromhon, and Gurvan Bulag faults), and Tibet (2001, Kunlun fault). Even the 1906 San Francisco earthquake had more than one hundred kilometers of faulting that occurred offshore. The postearthquake investigations of these events, particularly the classic studies of the San Andreas (Lawson, 1908) and Gobi-Altay (Florensov and Solonenko, 1965) have provided invaluable geomorphic and structural descriptions of long surface ruptures. However, the number of surface offset measurements has been relatively limited for even the best studied of these events. The 2002 Denali fault earthquake is similar to its predecessors in that it, too, occurred in a remote area, but with helicopter access we were able systematically to measure offset along the length of the rupture. We have also been able to build on the observations of past researchers with regard to the nature and variability of surface offset and the structural complexities to consider when measuring them. In this regard, we feel that the surface slip distribution presented here describes the coseismic surface deformation for this earthquake, both in amount and change along strike.

The 2002 Denali fault surface rupture shares basic structural characteristics with other large-slip historical strike-slip ruptures. On a large scale, the surface rupture is simple, narrow, and continuous. It occurred along existing scarps and other geomorphic indicators of prior faulting. On a small scale, the fault trace consists of left-stepping right-lateral rupture segments, each typically tens to many hundreds of meters long that usually have a north-side-up component of vertical slip. Locally the fault zone broadens where complexities result from changes in strike or rupture through thick unconsolidated deposits or glaciers. About one-third of the strike-slip surface rupture occurred through glacier ice. The ice fabric commonly influenced the expression of the fault at the surface and resulted in multiple fault strands parallel, and at a high angle to, internal ice fabric. Even with these complexities, offset glacier features provided mini-

mum slip values and at some sites perhaps a complete measure of surface slip.

The 2002 rupture provides insight into fault geometry at the intersections of large seismogenic faults and into rupture propagation. The Susitna Glacier thrust fault projects into the Denali fault at a 48° angle. Although the connection between the two is obscured beneath glacier ice, fractures from the faults lie within 400 m of one another and therefore likely intersect in the shallow subsurface. A 26-km-long transfer zone lies between the Denali and Totschunda faults along which rupture was discontinuous on both right-slip and normal faults. This transfer zone directly intersects the Denali fault at the surface at a 17° angle. Steps and bends in faults, and structural intersections between faults, have often been cited as features that might control the initiation or termination of rupture. They are also used as a basis for segmenting faults in seismic hazard analyses. Although three faults were involved in the Denali fault earthquake, our mapping indicates there are direct connections between adjacent ones. In this sense the rupture can be thought of as continuous, though geometrically variable, fault surface. The two fault intersections did not appear to have played any significant role in impeding the rupture, which simply propagated through them.

The surface slip distribution (Fig. 9) systematically records changes in the amount and location of slip that occurred during the dynamic, unilateral, west to east rupture on the Denali and Totschunda faults. We recognize four major sections of the slip on the strike-slip faults between the epicenter and the east end of the rupture on the Totschunda. These have typical offsets of 0 to 2 m (epicenter to km 42), 4 to 6 m (km 42 to km 174), 6 m to almost 9 m (km 174 to km 228), and 1 to 3 m (km 228 to km 302). In detail these can be subdivided into additional slip sections and slip steps. The change in the amount of slip across each slip step appears to occur over relatively short distances (2.7–4.7 km). One of the most interesting comparisons is the positive correlation of pulses of moment release and large accelerations with steps in the observed slip distribution. The largest strong-motion subevents occur between the east end of the Black Rapids Glacier and the TAPS, where surface slip ramps up from about 4 m to almost 6 m, and west of Gillett Pass, where slip increases from about 5 m to nearly 9 m.

The slip distribution for the Denali and Totschunda faults and the estimates of average surface offset derived from it (along with the value for the Susitna Glacier fault), allow calculation of a geological moment magnitude of M_w 7.8 for the 2002 Denali fault earthquake. This is in very good agreement with the seismologically determined value of **M** 7.9. An important task facing the paleoseismological community is the measurement of slip in prehistoric earthquakes. As demonstrated by the Denali fault earthquake rupture, surface slip measurements can provide for accurate calculations of earthquake magnitude. The paleo-offset data may also be used to calculate the magnitudes of past events. These calculations, coupled with information on changes in the amount of slip along strike in paleoevents, could provide a basis for advancing the modeling of strong ground motion in future large earthquakes.

Acknowledgments

We acknowledge the helpful discussions and interactions in the field with Gary Carver, Lloyd Cluff, Donna Eberhart-Phillips, Art Frankel, Jeff Freymueller, Sigrun Hreinsdóttir, Mike Metz, and George Plafker. Thanks also to the helicopter pilots who flew us around and kept us safe, in particular, Jon Laravee at Prism Helicopters. Thanks also to Charlie Rubin, Kerry Sieh, and Wes Wallace who participated in the postearthquake fieldwork in November 2002 and who generously contributed their field data to the compilation presented in this report. Field work was supported by the USGS and by a Cooperative Research and Development Agreement (CRADA) between the USGS, Alyeska Pipeline Service Company, and Pacific Gas and Electric Company. We thank W. D. Page, Tom Fumal, and Art Frankel for constructive reviews of the manuscript.

References

Bemis, S. P., and W. K. Wallace (2003). Active structures in the foothills of the north-central Alaska Range (abstract), *EOS* **84,** S12A-0380.

Brocher, T. M., G. S. Fuis, W. J. Lutter, N. I. Christensen, and N. A. Ratchkovski (2004). Seismic velocity models for the Denali fault zone along the Richardson Highway, Alaska, *Bull. Seism. Soc. Am.* **94,** no. 6B, S85–S106.

Brogan, G. E., L. S. Cluff, M. K. Korringa, and D. B. Slemmons (1975). Active faults of Alaska, *Tectonophysics* **29,** 73–85.

Clague, J. J. (1979). The Denali fault system in southwest Yukon Territory: a geologic hazard?, in *Current Research, Part 1, Geological Survey of Canada Paper 79-1A*, 169–178.

Crone, A. J., and M. N. Machette (1984). Surface faulting accompanying the Borah Peak earthquake, central Idaho, *Geology* **12,** 664–667.

Crone, A. J., S. F. Personious, P. A. Craw, P. J. Haeussler, and L. A. Staft (2004). The Susitna Glacier thrust fault—characteristics of surface ruptures on the fault that initiated the 2002 Denali fault earthquake, *Bull. Seism. Soc. Am.* **94,** no. 6B, S5–S22.

DeMets, C., R. G. Gordon, D. F. Argus, and S. Stein (1994). Effect of recent revisions to the geomagnetic reversal time scale on estimates of current plate motions, *Geophys. Res. Lett.* **21,** 2191–2194.

Eberhart-Phillips, D., P. J. Haeussler, J. T. Feymueller, A. D. Frankel, C. M. Rubin, P. Craw, N. A. Ratchkovski, G. Anderson, G. A. Carver, A. J. Crone, T. E. Dawson, H. Fletcher, R. Hanson, E. L. Harp, R. A. Harris, D. P. Hill, S. Hreindóttir, R. W. Jibson, L. M. Jones, R. Kayen, D. K. Keefer, C. F. Larsen, S. C. Moran, S. F. Personius, G. Plafker, B. Sherroed, K. Sieh, N. Sitar, and W. K. Wallace (2003). The 2002 Denali fault earthquake, Alaska: a large magnitude slip-partitioned event, *Science* **300,** 1113–1118.

Fletcher, H. J., and J. T. Freymueller (1999). New GPS constraints on the motion of the Yakutat block, *Geophys. Res. Lett.* **26,** 3029–3032.

Florensov, N. A., and V. P. Solonenko (1965) *The Gobi-Altay Earthquake (in Russian)*. Moscow, Akademiya Nauk USSR (English translation by Israel Program for Scientific Translations). Washington, D.C., U.S. Department of Commerce, 391 pp.

Frankel, A. (2004). Rupture process of the M 7.9 Denali fault, Alaska, earthquake: subevents, directivity, and scaling of high-frequency ground motions, *Bull. Seism. Soc. Am.* **94,** no. 6B, S234–S255.

Grantz, A. (1966). Strike slip faults in Alaska, *U.S. Geol. Surv. Open-File Rep. 267.*

Guatteri, M. G., and P. A. Spudich (1998). Coseismic temporal changes of slip direction: the effect of absolute stress on dynamic rupture, *Bull. Seism. Soc. Am.* **86,** 777–789.

Hanks, T. C., and H. Kanamori (1979). A moment magnitude scale, *J. Geophys. Res.* **84,** 2348–2350.

Hreinsdóttir, S., J. T. Freymueller, and R. Burgmann (2003a). Coseismic slip distribution of the Denali fault earthquake as estimated from GPS measurements (abstract), *EOS* **84,** S11H-07.

Hreinsdóttir, S., J. T. Freymueller, H. J. Fletcher, C. F. Larsen, and R. Bürgmann (2003b). Coseismic slip distribution of the 2002 M_w 7.9 Denali fault earthquake, Alaska, determined from GPS measurements, *Geophys. Res. Lett.* **30,** doi 10.1029/2003GL017447.

Ji, C., D. Helmberger, and D. Wald (2002). Preliminary slip history for the 2002 Denali earthquake, *EOS* **S72F,** 1344.

Kikuchi, M., and Y. Yamanaka (2002). Source rupture processes of the central Alaska earthquake of Nov. 3, 2002, inferred from teleseismic body waves (+ the 10/23 M 6.7 event), *EIC Seismological Note 129*, Earthquake Research Institute (ERI), University of Tokyo, Tokyo.

Lawson, A. C. (Chairman) (1908). *The California Earthquake of April 18, 1906: Report of the State Earthquake Investigation Committee, Vol. 1*, Carnegie Institution of Washington, Publication **87,** 434–448.

McGill, S. F., and C. M. Rubin (1999). Surficial slip distribution on the central Emerson fault during the June 28, 1992, Landers earthquake, California, *J. Geophys. Res.* **104,** 4811–4833.

Plafker, G., L. M. Gilpin, and J. C. Lahr (1994). Neotectonic map of Alaska, in *The Geology of Alaska: Plate 12, The Geology of North America*, G. Plafker and H. C. Berg (Editors), Geological Society of America, Boulder, Colorado, G-1.

Ratchkovski, N. A., R. A. Hansen, J. C. Stachnik, T. Cox, O. Fox, L. Rao, E. Clark, M. Lafevers, S. Estes, J. B. MacCormack, and T. Williams (2003). Aftershock sequence of the M_w 7.9 Denali fault, Alaska, earthquake of 3 November 2002 from regional seismic network data, *Seism. Res. Lett.* **74,** 743–752.

Reed, B. L., and M. A. Lanphere (1973). Alaska-Aleutian Range batholith; geochronology, chemistry, and relation to circum-Pacific plutonism, *Geol. Soc. Am. Bull.* **84,** 2583–2609.

Richter, D., and N. Matson (1971). Quaternary faulting in the eastern Alaska Range, *Geol. Soc. Am. Bull.* **82,** 1529–1539.

Ridgeway, K. D., J. M. Trop, W. J. Nokleberg, C. M. Davidson, and K. R. Eastham (2002). Mesozoic and Cenozoic tectonics of the eastern and central Alaska Range: progressive basin development and deformation in a suture zone, *Geol. Soc. Am. Bull.* **114,** 1480–1504.

Rockwell, T. K., S. Lindvall, T. E. Dawson, R. Langridge, W. Lettis, and Y. Klinger (2002). Lateral offsets on surveyed cultural features resulting from the 1999 Izmit and Düzce earthquakes, Turkey, *Bull. Seism. Soc. Am.* **92,** 79–94.

Schwartz, D. P., and Denali Fault Earthquake Geology Working Group (2003). Paleoearthquakes on the Denali-Totschunda fault system: preliminary observations of slip and timing (abstract), *EOS* **84,** S11B-03.

Sieh, K. E. (1977). A study of Holocene displacement history along the south-central reach of the San Andreas fault, *Ph.D. Dissertation*, Stanford University.

St. Amand, P. (1957). Geological and geophysical synthesis of the tectonics of portions of British Columbia, the Yukon Territory, and Alaska, *Geol. Soc. Am. Bull.* **68,** 1343–1370.

Thoms, E. E. (2000). Late Cenozoic unroofing sequence and foreland basin development of the central Alaska Range: implications from the Nenana Gravel, *Master's Thesis*, University of Alaska, Fairbanks.

Treiman, J. A., K. J. Kendrick, W. A. Bryant, T. K. Rockwell, and S. F. McGill (2002). Primary surface rupture associated with the M_w 7.1 16 October 1999 Hector Mine earthquake, San Bernardino County, California, *Bull. Seism. Soc. Am.* **92,** 1208–1226.

Weber, F. R., and D. L. Turner (1977) A late Tertiary thrust fault in the central Alaska Range, *U.S. Geol. Survey. Circular 751-B*, B66–B67.

Woodward-Lundgren and Associates (1974). Summary report basis for pipeline design for active-fault crossings for the Trans-Alaska Pipeline System, Appendix A-3.

Wright, T. J., Z. Lu, and C. Wicks (2003). Source model for the M_w 6.7, 23 October 2002, Nenana Mountain earthquake (Alaska) from InSAR, *Geophys. Res. Lett.* **30,** doi 10.1029/2003GL018014.

Appendix tables 1 and 2 follow.

U.S. Geological Survey
4200 University Drive
Anchorage, Alaska 99508
(P.J.H.)

U.S. Geological Survey, MS977
345 Middlefield Road
Menlo Park, California 94025
(D.P.S., T.E.D., H.D.S., J.J.L.)

U.S. Geological Survey
Department of Earth and Space Sciences
Box 351310
University of Washington
Seattle, Washington 98195
(B.S.)

Istituto Nazionale di Geofisica e Vulcanologia
Sismologia e Tettonofisica
Via di Vigna Murata 605
00143 Roma, Italy
(F.R.C.)

State of Alaska
Department of Natural Resources
Division of Geological and Geophysical Surveys
3354 College Road
Fairbanks, Alaska 99709
(P.A.C.)

U.S. Geological Survey, MS966
P.O. Box 25046
Denver, Colorado 80225-0046
(A.J.C., S.F.P.)

Manuscript received 13 April 2004.

Appendix 1

Table and Descriptions of Site Localities along the Denali and Totschunda Faults, 2002 Denali Fault Earthquake

Distance along DF/TF (from epicenter, km)	Latitude	Longitude	Date	Horizontal slip (cm)	Hz error (+) (cm)	Hz error (-) (cm)	Vertical (cm)	Vertical error (+) (cm)	Vertical error (-) (cm)	Vertical sense	Scarp azimuth	Dip	Fault zone width main zone (m)	Fault zone width total (m)	Glacier measurement	Fault	Observers	Field Note	Culled (Y/N)	Notes
0.000	63.52000	-147.53000	11/3/2002												no	DF			N	Epicenter
18.750	63.52907	-147.15781	11/7/2002	0											no	DF	TD/BS	DS01	N	Westernmost extent of observed rupture. Observed rupture extending through Susitna Glacier and over pass to West Fork Glacier. Horizontal offset arbitrarily assigned as zero.
20.510	63.53005	-147.12282	11/8/2002	160	50	50	67	20	20	SSU		70 S			yes	DF	PJH/PAC	PH269	N	Horizontal measurement based on offset matching surfaces on snowpack. Vertical measurement based on offset gravel layer in glacier ice. An inflection point on the edge of the snow scarp made a good piercing point. Chasm width was 0.5 m.
21.970	63.52863	-147.09372	11/8/2002	41	5	5	10	10	10	SSU					no	DF		k74	N	West of Sustina Glacier, in 1.4 m deep snow
22.180	63.52851	-147.08939	11/8/2002	119	25	25	20	5	5	SSU					no	DF		k75	N	Channel thalweg (snow covered)
23.220	63.52845	-147.06783	7/25/2003	140	10	10	22	4	4	SSU	101				no	DF	DS/PH/BS	HSS-605	N	Active drainage
24.830	63.52662	-147.03548	11/8/2002	297	20	20	50	5	5	SSU					no	DF		k77	Y	Offset stream channel edge. East side of tributary creek to westernmost Sustina Glacier.
25.310	63.52572	-147.02657	11/8/2002	205	50	50	77	40	40	SSU					no	DF	PJH/PAC	PH266	N	Horizontal and vertical offsets based on matching snow surfaces. Reported measurements are average of three measurements. Width of disturbed snowpack over fault zone was 1.5 m.
30.000	63.52092	-146.93420	11/8/2002	95	5	5	33	5	5	NSU		90 N			yes	DF	PJH/PAC	PH274	N	Pull apart matching surfaces in glacial ice. Very precise measurements on both glacier ice and snow surfaces.
33.450	63.52127	-146.86343	11/8/2002	96	5	5	42	5	5	SSU		61 S			yes	DF	PJH/PAC	PH276	N	Measurement taken in offset glacial ice features. Vertical measurement was offset snow features.
36.000	63.51799	-146.81413	11/7/2002				120			SSU					yes	DF	TD/BS	DS02	N	Vertical offset of ice on morraine of Susitna Glacier matching ash/glacial flour deposit. Crack in ice was near vertical and opening was 15-20 cm wide at base of scarp.
49.0-58.0	62.47871 to 63.49313	146.57954 to 146.42528		360	50	10										DF			N	GPS data from Hreinsdottir et al. (in prep.) collected at benchmarks along the Black Rapids Glacier. We consider this data superior to nearby measurements to the E on the glacier ice.
59.000	63.48542	-146.36713	11/8/2002	123	8	8	42	10	10	NSU		78 N			yes	DF	PJH/PAC	PH298	Y	Horizontal measurement based on offset corners in ice surface. One corner was broken so it was a bit hard to know exactly where they matched up (within 8 cm); vertical could be about 18 cm larger.
62.500	63.47815	-146.30062	11/8/2002	228	20	20	49	5	5	SSU					yes	DF	PJH/PAC	PH301	Y	Two vertical measurements, one in ice, one on snow. The snow surface one was better. Horizontal based on offset matching features.
68.080	63.46390	-146.19625	11/8/2002	390	5	5	106	5	5	NSU		80 N			yes	DF	PJH/PAC	PH305	N	Vertical measurement based on offset snow and ice features. Horizontal based on offset corners at edge of fault trace.
71.880	63.45587	-146.12280	11/8/2002	400	50	50	88	2	2	NSU					yes	DF	PJH/PAC	PH306	N	Another measurement of 2.8 m right-lateral offset was taken further to the east, with 0.5-1.0 m N side up offset. However, in the field we decided this measurements was better.
74.500	63.44988	-146.07325	11/8/2002	365	20	20	40	30	30	SSU		90 N			yes	DF	PJH/PAC	PH308	N	Offset ridge of glacial ice
78.000	63.43608	-146.0041	7/18/2003	385	50	50					290		2.8	10 - 12	no	DF	PH,HS,FC	03-211b	N	Stream channel and terrace riser.
80.000	63.43655	-145.43655	7/18/2003	480	40	80	160	50	50				3.2		no			03-213	N	
80.180	63.43652	-145.96337	7/18/2003	270	90	34					296		1 - 3	20	no	DF	PH,HS,FC	03-212	N	Small dry channel. 310W-50 is max, 236-304 is min for brittle faulting.
82.870	63.42550	-145.91357	11/9/2002	450	25	25									no	DF	CR/KS/GP	k80	N	West of 70 m mid-Holocene offsets in Augustana Creek drainage. Must be part of an older offset. Brush not disturbed.
83.560	63.42345	-145.89966	11/9/2002	410	30	30	60	5	5	NSU					no	DF	CR/KS/GP	k78	N	Offset on crest of small debris flow levee.
83.680	63.42313	-145.89854	11/9/2002	320	30	30	8	8	8	NSU					no	DF	CR/KS/GP	k79	N	Offset of thalweg of one meter wide gully
86.900	63.41277	-145.83783	7/15/2003	370	125	125					306		nr	nr	no	DF	PH,HS,FC	03-205	N	Edge of thicket and ridgeline
88.540	63.40507	-145.80965	11/3/2002	500	100	100	133	50	50	NSU					no	DF	PJH/PAC	PH031	N	Based on matching tears in tundra root mat. Measurement taken at juncture of chasm and push-up. Massive permafrost at a depth of about 1.1 m. Ground cracks to almost 4 m.
88.930	63.4043	-145.80283	7/15/2003	200	70	70	150	70	70	NSU			7	12	no	DF	PH,HS,FC	03-203	Y	Line of willows. Fault strike and vertical difficult to estimate
91.900	63.38827	-145.75484	11/9/2002	575	25	25	100	10	10	NSU			5		no	DF	CR/KS/GP	k92	Y	Offset of crest of west-facing terrace riser, on the east side of the Delta River.
92.120	63.38736	-145.75100	11/9/2002	180	20	20	35	10	10	NSU					no	DF	CR/KS/GP	k93	Y	Offset on base of channel wall, east of the previous measurement
93.230			11/3/2002	542											no			Alyeska	N	Alyeska Pipeline survey
93.330	63.38180	-145.73072	11/10/2002	390	30	30				NSU					no	DF		TDWW	N	Richardson Hwy centerline, no vertical determined due to repairs.
96.600	63.36812	-145.67244	7/16/2003	480	50	50							6.8		no	DF	TD/DS/PH	DS-03	N	Just west of K85 in next channel.
96.630	63.36823	-144.6731	7/16/2003	570	50	50									no	DF	TD/DS/PH	DHS-1	N	Remeasure of k85
96.630	63.36752	-145.67240	11/9/2002	630	30	30	100	10	10	NSU					no	DF	CR/KS/GP	k85	N	Offset on east-facing channel wall
96.930	63.36593	-145.66768	11/9/2002	504	25	25	71	5	5	NSU					no	DF	CR/KS/GP	k91	N	Offset of channel wall. Excellent measurement
96.930	63.36666	-145.6653	7/15/2003	446	29	18	23	2	3	NSU	50				no	DF	DS/TD/PM	DS-2	N	Gully in debris flow complex. Reoccupation of K91
96.935	63.36581	-145.66750	11/9/2002	415	50	50	36	5	5	NSU					no	DF	CR/KS/GP	k90	N	Offset on thalweg of small gully. This offset included a secondary trace, several meters upstream (to the south).
96.935	63.36657	-145.66632	7/16/2003	480	45	60				NSU	117				no	DF	TD/DS/PM	DS-2b	N	Channel edge
96.950	63.36568	-145.66710	11/9/2002	540	50	50	60	10	10	NSU					no	DF	CR/KS/GP	k89	N	Offset on crest of east-facing channel wall. Quality not as good as k85 or k88.
97.000	63.36546	-145.66631	11/9/2002	420	20	20	90	5	5	NSU					no	DF	CR/KS/GP	k88	N	Offset on crest of east-facing channel wall. We accounted for minor fracturing off of the main trace. Excellent measurement.
101.500	63.34825	-145.58605	11/8/2002	300	25	25	71	10	10	SSU		85 S			yes	DF	PJH/PAC	PH311	N	Offset crevasse measurment. Piercing point was edge of new snow at edge of crevasse.
102.900	63.34057	-145.56285	11/8/2002	352	20	20	205	20	20	SSU		76 S			yes	DF	PJH/PAC	PH312	N	Offset crevasse. Hung tape from top of overhanging offset crevasse wall to measure vertical.
102.950	63.34038	-145.56222	11/8/2002	450	50	50	180	50	50	SSU		73 S			yes	DF	PJH/PAC	PH313	N	Offset crevasse
104.740	63.33319	-145.53022	11/11/2002	510	20	20	55	10	10	SSU	294	60N			yes	DF	PJH/PAC	PH465	N	Offset crevasse, excellent piercing points, fault trace subparallel to glacier ice fabric
105.520	63.33077	-145.51508	11/11/2002	355	20	20	150	25	25	SSU	280	62N			yes	DF	PJH/PAC	PH466	Y	Offset crevasse, excellent piercing points, fault trace subparallel to glacier ice fabric, minimum value in stepover
106.380	63.32815	-145.49937	11/11/2002	162	5	5	60	5	5	SSU	286	68N			yes	DF	PJH/PAC	PH468	Y	Offset crack on glacier ice, fault trace subparallel to glacier ice fabric; 1600 m E of last site; total throw measurement was excellent, minimum value in stepover

Latitude and longitude reported in WGS 84 datum.

This table updates and supercedes the supplementary online material found in Eberhart-Phillips *et al.* (2003).

(*continued*)

Appendix 1 (*continued*)

Distance along DF/TF (from epicenter, km)	Latitude	Longitude	Date	Horizontal slip (cm)	Hz error (+) (cm)	Hz error (-) (cm)	Vertical (cm)	Vertical error (+) (cm)	Vertical error (-) (cm)	Vertical sense	Scarp azimuth	Dip	Fault zone width main zone (m)	Fault zone width total (m)	Glacier measurement	Fault	Observers	Field Note	Culled (Y/N)	Notes
108.290	63.31592	-145.47076	11/11/2002	380	4	4	30	20	20	NSU					yes	DF	PJH/PAC	PH483	N	Pull-apart measurement on glacier ice; fault appeared to be paralleling medial moraine here. Only slickensides observed on glacier ice here, on N side at depth of 4 m. Anchorage Daily News headline photo locality
124.050	63.27098	-145.17417	11/11/2002	600	50	50	70	40	40	SSU	297	90			yes	DF	PJH/PAC	PH525	N	Pull-apart in glacier ice; matching rhombehedral faces in opening; very deep crack (~40 m) that narrows at great depth.
125.320	63.26580	-145.15153	11/11/2002	285	50	50	30	15	15	SSU	120				yes	DF	AC/SP	PC04	N	Offset ridge between crevasses; ridge about 10 m wide, rupture zone narrow and well defined except for snow-filled splay with little apparent displacement 10 m to south; offset of crevass edge appeared similar, but too dangerous to measure.
131.050	63.24934	-145.03543	11/11/2002	470	100	100	50	30	30	NSU	120				yes	DF	AC/SP	PC02	N	Measured from two strands across snow filled curved crevass. Combined data from PC02 and PC03.
134.600	63.23967	-144.97883	7/17/2003	465	15	15					127		5 - 10		yes	DF	PH,HS,FC	03-211a	N	Offset crevasses, note 03-211a is different locality than 211b
137.500	63.23069	-144.92382	7/17/2003	580	240	0					264		3.6		no	DF	PH,HS,FC	03-209	N	Channel in stagnating ice.
138.000	63.22892	-144.91458	7/17/2003	760	40	50					314		3 - 5		no	DF	PH,HS,FC	03-208	Y	Apparent snow field offset, probably an overestimate due to narrowing of field downslope.
138.590	63.2261	-144.90442	7/17/2003	715	65	75				NSU	314				no	DF	PH,HS,FC	03-207	N	Channel offset. Re-evaluation of adjacent channels indicates this is a two-event offset.
138.591	63.22619	-144.90443	7/7/2004	370	60	50									no	DF	TD/PH/DS	Stop 98	N	Swale 10 m east of apparent 7m offset (03-207)
138.680	63.22454	-144.89892	7/7/2004	260	40	60									no	DF	TD/PH/DS	Stop 99	Y	Thalweg of channel. Center of channel is well-defined, but location is in an area of numerous large left steps. Offset is probably a minimum.
138.690	63.22454	-144.89855	7/7/2004	260	80	60									no	DF	TD/PH/DS	Stop 100	Y	Thalweg of channel measured across a 10.8 meter-wide zone of 4-5 individual shears. Measurement is in a zone of large left steps and is probably a minimum.
139.940	63.2215	-144.87903	7/7/2004	320	50	40									no	DF	TD/PH/DS	Stop 102	N	Offset channel margin in coarse stream deposits. Eastern side of well-defined channel. Fault zone is narrow.
142.140	63.21205	-144.84026	7/17/2003	460	10	10	60	5	5	NSU	127		1.6	5.1	no	DF	TD/DS/PH	DS-10	N	Offset moraine.
142.300	63.21153	-144.83754	7/17/2003	455		35				NSU	136		2.7	14	no	DF	TD/DS/PM	DS-12	N	Small gulley.
142.570	63.21064	-144.83272	7//18/2003	470	20	20					120		nr	nr	no	DF	TD/DS/PM	DS-20	N	Channel margin. Feature is normal to fault strike
142.590	63.21045	-144.83245	7/18/2003	510	10	10	56			NSU	120		1		no	DF	TD/DS/PM	DS-21	N	Well defined gully crest. Very narrow fault zone
143.170	63.2084	-144.8216	7/18/2003	532	20	20				NSU	120		5.15		no	DF	TD/DS/PM	DS-22	N	Debris flow channel margin. Feature into fault 44, and 40 degrees
143.220	63.20833	-144.82066	7/18/2003	490	45	70				NSU	129		2		no	DF	TD/DS/PM	DS-23	N	West margin of debris flow channel. 1 drainage east of DS-22
143.520	63.20674	-144.81806	7/18/2003	480	50	50				NSU	124				no	DF	TD/PM	DS-24	N	Channel thalweg, near west margin Chistochina Gl.
143.750	63.20634	-144.81082	7/18/2003	445	40	40					309			10 - 15	no	DF	PH,HS,FC	03-215	N	Offset stream bank
146.770	63.19198	-144.75837	11/3/2002	450	150		0	30	0	NSU					no	DF	PJH/PAC	PH036	N	Offset of channel bank. Estimated offset from snowpack surface. Offset is a minimum. There was drag over at least 10 m on the hanging wall side of the fault. We estimated an offset of around 6 m with the drag. >330 (600?)
147.700	63.1889	-144.7428	7/19/2003	455	10	10	25	5	5	NSU	124				yes	DF	DS/PM/FC	7/19-1	N	Offset crevasse
151.457	63.16198	-144.66165	11/3/2002	170	30	30	33	20	20	NSU					no	DF	PJH/PAC	PH037	Y	Vertical measurement was based on offset of snow surfaces. Snowpack was particularly hard here. There was possibly another 0.25 m of offset just 2 m to the north. Bank consisted of gravel with a silty matrix.
157.100	63.14911	-144.57848	7/20/2003	450	35	35				NSU	129				no	DF	DS/PM/FC	7/19-3	N	Moss lined channel edge.
157.720	63.14725	-144.56769	11/7/2002	480	50						90				no	DF	TD/BS	DS03	N	Maximum is likely from multiple ruptures. Same location as K94 and 03-216
157.720	63.14782	-144.56557	7/19/2003	510	20	20	70	20	20	NSU	122		2.5	6	no	DF	TD/HS/JL	3-216	N	Channel edge
157.720	63.14782	-144.56557	7/19/2003	550	70	70	70	20	20	NSU	122				no	DF	TD/HS/JL	03-216b	N	Small terrace riser, a few meters east of 03-216
157.720	63.14725	-144.56769	11/10/2002	530	30		53	10	10		335				no	DF	CR/KS/GP	K94	N	
163.540	63.12354	-144.4638	7/18/2003	360	125	0				J	310		4 - 5		no	DF	TD,HS,JL	03-217	N	Offset road, hard to estimate due to road curvature
166.240	63.11147	-144.41722	11/10/2002	715	15		48	10	10		282				no	DF	CR/KS/GP	K95	Y	Horizontal offset could be 1 m less if extrapolate offset from beyond the mole track.
166.240	63.11185	-144.41517	7/18/2003	450	50	50	50	10	10	NSU	315				no	DF	TD,HS,JL	03-219	N	Channel margin, just west of pressure-ridge. This supercedes K95, which is a miscorrelation
166.400	63.11060	-144.41455	11/7/2002	290	20	20	68	10	10	NSU	96				no	DF	TD/BS	DS04	Y	Vertical offset on top of snow on both sides of creek; horizontal offset is on west side of creek bank
166.400	63.11060	-144.41455	7/19/2003	310	20	20	94	6	6	NSU	121				no	DF	TD,HS,JL	03-218	Y	Channel edge. Same as DS04 from Nov. This is a minimum value for total slip due to left step with pressure ridge just west of channel
169.900	63.09625	-144.35306	7/20/2003	345	25	25	134	5	5	NSU	312		5		no	DF	TD/PH/DS	DS-301	N	Offset stream. Excellent.
170.610	63.09332	-144.34058	11/10/2002	680	20	20	13	1	1	NSU	0-20				no	DF	CR/KS/GP	K97	Y	Slana R. excellent according to Sieh's notes.
170.610	63.09332	-144.34058	11/10/2002	280	20	20	90	5	5						no	DF	CR/KS/GP	K98	Y	Slana R. Astonishingly low according to Sieh's notes and may be missing traces.
170.910	63.09151	-144.33569	11/7/2002	510	50	50					100			15	no	DF	TD/BS	DS06	N	Streambank on western side of channel. 15m wide zone of deformation - possibly two traces that ruptured at once.
173.000	63.08630	-144.29506	11/10/2002	465	70	70	35	10	10						no	DF	CR/KS/GP	K100	N	Offset cutbank in gravel
173.780	63.08179	-144.28318	7/7/2004	540	40	30				NSU					no	DF	TD/PH/DS	Stop 104	N	Subtle terrace riser on west side of active channel, eastern side of larger channel.
174.200	63.08009	-144.27557	7/20/2003	645	50	60	180	10	10	NSU	304		5		no	DF	TD/PH/DS	DS-300	N	Channel margin on fan
175.720	63.07461	-144.24818	7/7/2004	730	30	85				NSU					no	DF	TD/PH/DS	Stop 103	N	Offset channel margin. This is the sum of four individual shears from north to south: 110cm, +10, -10cm; 160cm, +10, -25cm; 410cm, +10, -50cm; and 20cm
176.923	63.05269	-144.17605	11/3/2002	520	100	100	120	40	40	NSU					no	DF	PJH/PAC	PH046	N	Right-lateral offset of stream.
180.200	63.05513	-144.1709	7/24/2003	770	0	50				NSU	130		2.7		no	DF	DS/TD	DS-503	N	Offset crest of debris flow, Near DS-502 exposure.
182.000	63.04757	-144.13999	7/21/2003	750	0	160				NSU	123				no	DF	TD/DS/AM	Jack Cr-1	N	Offset stream, very sharp edge.
182.660	63.04440	-144.12678	11/7/2002	720	50	50					87				no	DF	TD/BS	DS07	N	Best measurement is on west side of stream channel
182.660	63.04493	-144.12762	7/24/2003	790	10	10					111		2.5		no	DF	DS/TD	DS-501	N	Channel offset.
184.270	63.03857	-144.0997	7/24/2003	810	0	25				NSU	120		1.5		no	DF	DS/TD	DS-500	N	Narrow single trace, very clean offset
186.190	63.02932	-144.06738	11/8/2002	800	75	75	150	20	20	NSU	97				no	DF	BLS/TD/WW	DS08	N	Offset stream and levee bar. We measured offset of levee bar crest.
189.440	63.01445	-144.01228	11/8/2002	680	50	50					76				no	DF	BLS/TD/WW	DS09	N	Offset edge of avalanche chute/stream channel; uphill facing scarp.
191.470	63.00595	-143.97690	11/8/2002	720	20	20					104				no	DF	BLS/TD/WW	DS10	N	Small stream bank with very well preserved channel edges that we could match up easily.
195.900	62.9869	-143.8984	7/21/2003	637	30	30	40	30	30	NSU	323				no	DF	HS,PH	03-220	N	Offset game trail

Appendix 1 (*continued*)

Distance along DF/TF (from epicenter, km)	Latitude	Longitude	Date	Horizontal slip (cm)	Hz error (+) (cm)	Hz error (-) (cm)	Vertical (cm)	Vertical error (+) (cm)	Vertical error (-) (cm)	Vertical sense	Scarp azimuth	Dip	Fault zone width main zone (m)	Fault zone width total (m)	Glacier measurement	Fault	Observers	Field Note	Culled (Y/N)	Notes
198.000	62.97697	-143.86637	11/8/2002	550	10	10					90				no	DF	BLS/TD/WW	DS11	N	Bone Creek. NW side of stream channel clearly offset by fault. Flooding of vegetated area on SE side of stream on south side of fault suggests slight vertical movement or shaking-induced settlement.
198.000	62.97697	-143.86637	7/24/2003	660	40	50					322				no	DF	HS,PH	03-227	Y	Bone Creek, same as DS-11. Probably not as well-constrained as the measurement taken in Nov due to stream deposition.
202.000	62.95811	-143.79849	11/8/2002	630	10	10					109				no	DF	BLS/TD/WW	DS12	N	Root/log embedded in streambank ripped apart by fault and offset RL.
205.280	62.94147	-143.74496	11/7/2002	550	50	50	95	15	15	SSU					no	DF	CR/KS/GP	SRP 3	N	Mentasta Road: driveway going into chapel, used center snow berm on dirt road.
205.300	62.94154	-143.74582	11/7/2002	554	60	60	130	10	10	NSU	N88E				no	DF	CR/KS/GP	SRP 2	N	Offset snowy trail, near Mentasta Road, 75 m north of chapel. Vertical scarp preserves two events (?), total scarp height about 3.0 m. Plunge on slip vector, 27 degrees.
210.600	62.91858	-143.65295	11/8/2002	470	15	15	80	10	10	NSU	123				no	DF	CR/KS/GP	SRP 1	Y	Tok Cutoff road
210.600	62.91858	-143.65295	11/4/2002	690	100	100									no	DF	PJH/PAC	PH184	N	Offset highway. 5.0 m offset measured directly; 1.9 m added from 500-m-wide zone of drag on N side. Vertical offset is small <1m. Vertical not measured because block just south of fault had tilted north and down.
213.740	62.90812	-143.59507	11/8/2002	690	30	30					108				no	DF	BLS/TD/WW	DS13	N	Steep-walled stream bank (west side) offset and stream channel blocked by pressure ridge.
215.420	62.90146	-143.5658	7/21/2003	450	125	125	160	20	20	NSU	310		4		no	DF	HS,PH	03-221	N	Offset game trail
223.300	62.86455	-143.43424	11/8/2002	550	75	75					96				no	DF	BLS/TD/WW	DS14	N	Huge fissure on ridgetop. Fissure is about 4m wide and 4m deep. We matched up fissure edges and measured displacement. Similar fissures on ridges to east and west of this site.
227.000	62.83716	-143.38303	11/10/2002	200	50	50					215				no	DF	AC/SP/BS	PCS02a	Y	Offset Spruce root on a long linear crack running up ridge - looks like a stepover fault from main strand, stepping over from the Denali on the east to the Totschunda on the west side of the valley. In step-over, may need to be summed
227.000	62.83716	-143.38303	11/10/2002	300	10	10	25	10	10	WSU	215				no	DF	AC/SP/BS	PCS02b	Y	Offset spruce root about 10m north of previous PCS02 measurement (in same fissure). In step-over, may need to be summed
227.000	62.83495	-143.38521	11/10/2002	275	20	20	55	10	10	WSU	190				no	DF	AC/SP/BS	PCS06	Y	Offsets of two sets of roots, both gave same offset (275 cm). In step-over, may need to be summed
227.200	62.84336	-143.37308	11/9/2002	490	75	75	200	30	30	SSU	93				no	DF	BLS/TD/WW	DS22	N	Fissure pull-apart with RL offset and large component of vertical offset. We matched up sides of the fissure for piercing points - fissure is about 5m and 2 m wide. Permafrost starts about 3m below ground surface.
227.200	62.84336	-143.37308	11/9/2002	680	10	10	120	5	5	SSU	93				no	DF	BLS/TD/WW	DS23	Y	Offset spruce root. This measurement comes from just east of TS22 in same fissure as TS22. Cracks in the ground nearby likely mean the slip measured here is a minimum.
229.000	62.831	-143.3451	7/21/2003	240	25	25					320		1.5	45	no	DF	HS,PH	03-222	N	Offset tree in DF/TF stepover zone
233.820	62.79840	-143.30693	11/9/2002				34	2	2	ESU	175				no	TF	BLS/TD/WW	DS26	N	Small but continuous rupture (several km) but little to no lateral offset.
235.540	62.78546	-143.28603	7/22/2003	108						NSU	319				no	TF	DS/PH	HS-500	N	Moss vegetation mat, in DF-TF stepover
239.000	62.75851	-143.25360	11/10/2002	0	10	10	95	20	20	NSU	139				no	TF	AC/SP/BS	PCS04	Y	Normal fault scarp that parallels the Totschunda trace but is on the NE side of the Little Toschunda Valley. Slope with mature trees adjacent to rupture looks like a colluvial wedge that was faulted in the Nov 3 event. Total scarp height is about 430 cm.
239.150	62.75684	-143.25304	11/10/2002	130	50	50	270	10	10	ESU	37				no	TF	AC/SP/BS	PCS03	N	Game trail crossing scarp has left-lateral offset. This location is about 100m SE of bend in fault. The fault crosses the creek and then heads east.
239.380	62.75448	-143.25613	11/9/2002	60	20	20	265	5	5	ESU	160				no	TF	BLS/TD/WW	DS21	N	Scarp cutting across Little Tok River on transfer fault between one rupture running up east side of valley that then jumps over to another structure running up the west side of the valley (which presumably joins the Totshunda fault).
240.000	62.74940	-143.25068	11/9/2002	100	5	5	70	5	5	ESU	147				no	TF	BLS/TD/WW	DS29	N	Spruce root ripped apart by the rupture that had RL oblique slip. Fissure in permafrost is very deep and narrow (50 cm wide).
242.380	62.72920	-143.23463	11/9/2002	133	5	5	38	2	2	ESU	152				no	TF	BLS/TD/WW	DS31	N	Offset spruce root.
248.600	62.68141	-143.17241	11/11/2002	170	2	2	12	3	3	SSU	328	90			no	TF	PJH/PAC	PH624	N	Excellent measurements from offset broken in half cobbles. Slope colluvium overlying stagnated layered glacier ice.
249.920	62.67313	-143.15265	7/22/2003	280	20	0	45	15	15	NSU	136		2.5	nr	no	TF	PH/DS	HS-557	N	Offset channel margin.
260.460	62.60522	-143.00994	11/10/2002	210	25	25	0	10	0	NSU	146				no	TF	AC/SP/BS	PCS05	N	Offset linear stream channel (west edge) in Platinum Creek drainage. Upvalley reach of channel is linear for about 40m and downvalley reach is linear for about 15m (far field view of offset projected across fault).
265.800	62.57190	-142.93580	7/22/2003	185	20	20					329		1 - 2	3	no	TF	TD,HS,JL	03-224	N	Offset gully
266.100	62.56996	-142.93174	7/23/2003	160	15	15					138				no	TF	TD,JL	TF-11	N	Offset gully. Just west of 03-224.
268.560	62.5534	-142.8998	7/23/2003	300	30	30				NSU	311		4	12	no	TF	DS/HS	03-225	N	
270.260	62.54205	-142.87755	7/23/2003	250	95	95					318				no	TF	TD,JL	TF-14	N	Stream offset. Poor Quality
271.000	62.51863	-142.82665	7/23/2003	310	20	70					325				no	TF	PH/BS	PB567	N	Nearby boulder channel offset 2.8-3.9 (3.3)m.
273.380	62.52202	-142.83575	11/4/2002	210	30	30	25	25	0	NSU					no	TF	PJH/PAC	PH116	N	3 m deep crack, water seeped from 1 m depth in crack and then froze.
276.770	62.49852	-142.79344	11/9/2002	175	10	10	20	10	10	SSU	145				no	TF	SFP/AJC	PC01	N	Horizontal slip value based on average of three measured values of torn forest floor. Precise location of measurement is on forest floor about 10 m northwest of northwest bank of tributary drainage of Totschunda Creek.
297.000	62.34583	-142.59642	11/4/2002	65	25	25	25	10	10	SSU					no	TF	PJH/PAC	PH101	N	Offset of cut bank. The thrust estimate there was poor because the surface was blocky and uneven. However, in an inactive channel frozen gravel and sand was thrust over snow 1.2 m.
300.100	62.32375	-142.56058	7/24/2003	100	45	20				SSU			1.5	4	no	TF	DS/HS	03-226	N	
302.000	62.3275	-142.57815		0											no	TF			N	Eastern end of rupture

Vertical sense: north side up, NSU; south side up, SSU; east side up, ESU; west side up, WSU. Fault: Denali fault, DF; Totschunda fault, TF.

Appendix 2

Table of Locations of Discontinuous Ground Cracking along the Denali Fault

Appendix 2: Observations of discontinuous ground cracking along the Denali fault					
Distance along DF/TF (from epicenter, km)	Latitude (°N)	Longitude (°E)	Date	Field Number	Notes
-1.250	63.511590	-147.560090	7/19/2003	SGSP08	Near east end of zone of discontinuous cracks, 2-10 m long, over a 200 m distance. At base of E-W trending 1-2 m NSU paleoscarp. Cracks on tundra soils and bouldery talus on relatively flat ground. Right-lateral slip of 2±1 cm and 1 cm south side down.
-2.360	63.508950	-147.580340	7/19/2003	SGSP10	Small cracks with <10cm south side down offset. 100-200 m length of discontinuous cracks along base and across face of 1-2 m high NSU paleoscarp. No lateral slip.
-2.56	63.508550	-147.582533	7/3/2004	419	Discontinuous fractures
-2.75	63.508417	-147.585933	7/3/2004	431	Discontinuous fractures
-3.14	63.508167	-147.594017	7/3/2004	432	Discontinuous fractures
-3.18	63.508117	-147.594567	7/3/2004	440	Discontinuous fractures
-4.61	63.508867	-147.623783	7/5/2004	487	Discontinuous 5-m-long fractures in wet area.
-4.63	63.508783	-147.624150	7/5/2004	489	Discontinuous 5-m-long fractures in wet area, with no adjacent topography.
-5.10	63.508667	-147.633333	7/4/2004	458	Fractures with downslope movement. Lie within 5 m of surface trace. Sand blows along cracks in a wet area about 15 m long.
-6.41	63.508750	-147.660033	7/5/2004	490	Discontinuous fractures along fault trace observed from the air.
-6.60	63.508717	-147.660533	7/5/2004	491	Discontinuous fractures along fault trace observed from the air.
-18.20	63.495700	-147.894450	7/4/2004	474	Discontinuous fractures along fault trace observed from the air.
-21.04	63.489833	-147.950433	7/3/2004	450	Discontinuous fractures along fault trace observed from the air.
-23.81	63.487350	-148.005917	7/4/2004	475	Discontinuous fractures along fault trace observed from the air.
-24.15	63.486967	-148.012500	7/4/2004	476	Discontinuous fractures on bench and pressure ridge adjacent to linear swale that defines the Denali fault trace.
-32.36	63.484950	-148.177517	7/4/2004	484	Discontinuous fractures along fault trace observed from the air.
-34.95	63.482317	-148.229133	7/4/2004	485	Associated with adjacent downslope movement. Another 20-m-long crack was located on the fault trace, and it traversed down a dry and broad west-facing slope. This crack locally had up to 5 cm right-lateral offset.
-55.38	63.462140	-148.639080	8/12/2004	PC2	Slope failure—east end.
-55.49	63.461140	-148.640880	8/12/2004	PC1	Slope failure—west end.
-56.10	63.461730	-148.653490	8/12/2004	PC3	Crack with a sand blow in a sag pond.